

Review

Compressive Strength of Sustainable Geopolymer Concrete Composites: A State-of-the-Art Review

Hemn Unis Ahmed ^{1,2,*} , Azad A. Mohammed ¹, Serwan Rafiq ¹, Ahmed S. Mohammed ¹ , Amir Mosavi ^{3,4,5,*} , Nadhim Hamah Sor ^{6,7}  and Shaker M. A. Qaidi ⁸ 

- ¹ Civil Engineering Department, College of Engineering, University of Sulaimani, Kurdistan Region, Sulaimaniyah 46001, Iraq; azad.mohammed@univsul.edu.iq (A.A.M.); serwan.rafiq@univsul.edu.iq (S.R.); ahmed.mohammed@univsul.edu.iq (A.S.M.)
- ² Department of Civil Engineering, Komar University of Science and Technology, Kurdistan Region, Sulaimaniyah 46001, Iraq
- ³ Institute of Software Design and Development, Obuda University, 1034 Budapest, Hungary
- ⁴ Department of Informatics, J. Selye University, 94501 Komarno, Slovakia
- ⁵ Institute of Information Society, University of Public Service, 1083 Budapest, Hungary
- ⁶ Civil Engineering Department, University of Garmian, Kurdistan Region, Kalar 46021, Iraq; nadhim.abdulwahid@garmian.edu.krd
- ⁷ Department of Civil Engineering, Harran University, 63050 Sanliurfa, Turkey
- ⁸ Department of Civil Engineering, College of Engineering, University of Duhok, Kurdistan Region, Duhok 42001, Iraq; shaker.abdal@uod.ac
- * Correspondence: hemn.ahmed@univsul.edu.iq (H.U.A.); amir.mosavi@mailbox.tu-dresden.de (A.M.)



Citation: Ahmed, H.U.; Mohammed, A.A.; Rafiq, S.; Mohammed, A.S.; Mosavi, A.; Sor, N.H.; Qaidi, S.M.A. Compressive Strength of Sustainable Geopolymer Concrete Composites: A State-of-the-Art Review. *Sustainability* **2021**, *13*, 13502. <https://doi.org/10.3390/su132413502>

Academic Editor: Quoc-Bao BUI

Received: 14 October 2021

Accepted: 15 November 2021

Published: 7 December 2021

Publisher's Note: MDPI stays neutral with regard to jurisdictional claims in published maps and institutional affiliations.



Copyright: © 2021 by the authors. Licensee MDPI, Basel, Switzerland. This article is an open access article distributed under the terms and conditions of the Creative Commons Attribution (CC BY) license (<https://creativecommons.org/licenses/by/4.0/>).

Abstract: The building industry, which emits a significant quantity of greenhouse gases, is under tremendous pressure due to global climate change and its consequences for communities. Given the environmental issues associated with cement production, geopolymer concrete has emerged as a sustainable construction material. Geopolymer concrete is an eco-friendly construction material that uses industrial or agricultural by-product ashes as the principal binder instead of Portland cement. Fly ash, ground granulated blast furnace slag, rice husk ash, metakaolin, and palm oil fuel ash were all employed as binders in geopolymer concrete, with fly ash being the most frequent. The most important engineering property for all types of concrete composites, including geopolymer concrete, is the compressive strength. It is influenced by different parameters such as the chemical composition of the binder materials, alkaline liquid to binder ratio, extra water content, superplasticizers dosages, binder content, fine and coarse aggregate content, sodium hydroxide and sodium silicate content, the ratio of sodium silicate to sodium hydroxide, the concentration of sodium hydroxide (molarity), curing temperature, curing durations inside oven, and specimen ages. In order to demonstrate the effects of these varied parameters on the compressive strength of the fly ash-based geopolymer concrete, a comprehensive dataset of 800 samples was gathered and analyzed. According to the findings, the curing temperature, sodium silicate content, and alkaline solution to binder ratio are the most significant independent parameters influencing the compressive strength of the fly ash-based geopolymer concrete (FA-BGPC) composites.

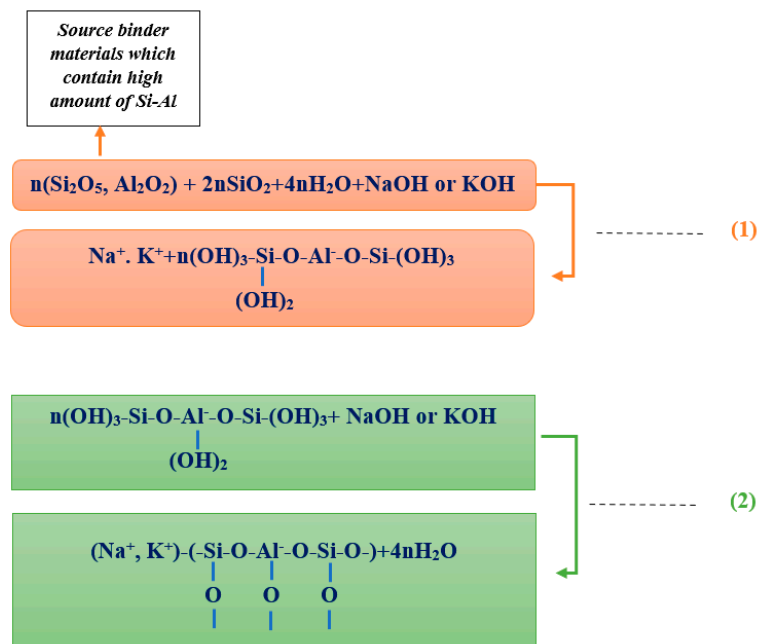
Keywords: geopolymer concrete; mix proportion; fly ash; compressive strength; curing; alkaline solution; sustainable concrete; sustainability; circular economy; composite materials design

1. Introduction

It is well known that the production of Portland cement necessitates a significant amount of energy and, at the same time, contributes to the release of a large amount of total carbon dioxide (around 7%) into the atmosphere, both directly and indirectly [1]. The direct release of CO₂ is called calcination, while the indirect release of CO₂ is caused by burning fossil fuels to heat the kiln and quarrying and transporting the cement [2,3]. In addition, one ton of cement requires around 2.8 tons of raw materials; this is a resource-depleting process

that consumes a vast number of natural resources such as limestone and shale for the manufacturing of cement clinkers [4]. Furthermore, the concrete industry requires around one trillion liters of mixing water every year [5]. Behind aluminum and steel manufacturing, the cement sector is the most energy-intensive construction material in the same lines. Each ton of cement produced in a typical cement factory consumes roughly 110–120 kWh [6]. However, on the other hand, cement-based concrete is still the most widely utilized material in the building industry worldwide [7]. Therefore, a highly efficient application of renewable and non-renewable raw materials is essential for economic development [8]. As the world continues to face major environmental concerns, developing a unique material to replace Portland cement has become increasingly important [9,10].

A convenient, suitable replacement to conventional concrete is geopolymer technology developed first by Davidovits in France, 1970 [11]; the ancient Roman civilizations used geopolymer to build their monumental and castles in ancient times [12]. Geopolymers are inorganic aluminosilicate polymers made by activating various aluminosilicate minerals with different alkaline solutions [13]. Geopolymer materials have an amorphous microstructure and chemical components similar to natural zeolitic materials [14]. The chemical reaction between alkaline solution and source binder material which contains aluminosilicate is called polymerization process; a polymeric chain and ring structure comprised of Si-O-Al-O linkages is produced during the polymerization process as shown in Scheme 1, the scheme is adapted from [15], with an empirical formula of $\{Mn[-(SiO_2)_z-AlO_2]n \cdot wH_2O\}$, where M is an alkali action, n is the percent of polymerization, and w is the content of water [14]. In addition, the chains in aluminosilicate could be in the form of poly-(sialate) with the ratio of Si to Al being equal to 1.0 (-Al-O-Si- chain), poly (sialate-siloxo) with the ratio of Si to Al being equal to 2.0 (-Al-O-Si-Si- chain), and poly (sialate-disiloxo) with the ratio of Si to Al being equal to 3.0 (-Al-O-Si-Si-Si- chain) [16].



Scheme 1. Chemical reactions during geopolymerization process.

The following is a quick explanation of how geopolymerization process works. In the first stage, the dissolution of the binder's silicate and aluminum elements inside the high alkalinity aqueous solution produces silicon and aluminum oxide ions. After that, a mixture of silicate, aluminate, and aluminosilicate species is used in the second stage, which is further condensed through a simultaneous poly-condensation-gelation operation, and finally, an amorphous gel is produced [17]. The type of source binder materials, concentration of alkaline solution, molarity of sodium hydroxide, ratio of sodium

silicate to sodium hydroxide, extra water, mixture proportions, and curing process can all affect the performance of geopolymer concrete [18,19]. Moreover, the end output of the geopolymerization process is influenced by the chemical composition of the source binder materials ash-based geopolymer and the alkaline activator, which is frequently accelerated at higher temperatures [20,21]. Thus, after lime and cement, the geopolymer can be considered the third generation of cementing ingredients [22], and it is an eco-friendly and green material that has low green gas emission of around 70% lower than the Portland cement concrete due to the high consumption of by-product materials inside their mix proportions [23]. The mixed proportions of the geopolymer concrete consist of aluminosilicate binder, fine and coarse aggregates, alkaline solutions and water, and finally, a solid concrete formed from the polymerization of these components, which is quite similar to the typical conventional concrete [24]. Alumino-silicate-rich materials such as fly ash (FA), ground granulated blast furnace slag (GGBFS), rice husk ash (RHA), metakaolin (MK), silica fume (SF), red mud (RM), and palm oil fuel ash (POFA), or any hybridization of these ashes with or without Portland cement are used as geopolymer concrete binder materials. The performance and reactivity of these source binder materials are mainly dependent on their chemical composition, fineness, and glassy phase content, as presented in our former work [25]. Because of its low cost, wide availability, and increased potential for geopolymer preparation, fly ash is the most widely used source binder material for creating geopolymer concrete [26]. Fly ash is the finely chopped residue produced from the combustion of pulverized coal. It is imparted from the combustion chamber by using exhaust gages by electrostatic precipitators or other devices to filtrate the particles before the flue gages reach the chimneys [27,28]. Generally, based on the source of the coal being burned, FA is divided into two classes, namely class F fly ash which is produced from burning anthracite or bituminous coal, and class C fly ash which is mainly made from the burning of lignite coal sources, the former type has lower calcium content compared to class C fly ash [29]. Further, the main components of FA have typically consisted of SiO_2 , Al_2O_3 , Fe_2O_3 , and CaO with a lower percent of some other minerals, which is shown in Table 1. The total percent of SiO_2 , Al_2O_3 , and Fe_2O_3 for the class F fly ash is over 70%, with the content of CaO less than 10%, while for the class C fly ash total content of SiO_2 , Al_2O_3 , and Fe_2O_3 should be between 50% to 70% with the percent of CaO greater than 20% [30,31]. In addition, FA is considered a dangerous material because it contains many trace elements, such as Mn, Ti, Cr, V, Co, As, Pb, and Mo. The intensity of the toxic trace elements in FA could be 5–10 times greater than those in the raw material sources [32–34], and it has small amounts of polycyclic aromatic hydrocarbon and dioxins [35,36]. Therefore, the erroneous discarding of FA and any other by-product or waste materials will increase land occupation and destroy the environment and ecology [37–39]. Thus, to tackle these problems of FA and any other waste materials, efforts have been made towards re-use of them in an efficient and green way; for instance, high volumes of FA have been used to replace Portland cement in different types of concrete and cementitious composites [40–47]. More recently, FA has been utilized as an alternative source to make geopolymer paste [48,49], mortar [50,51], and concrete [52–54].

For the production of FA-BGPC, some reactions take place between alkali liquids and fly ash, and condensation among the resultant of Al^{3+} and Si^{4+} patterns, followed by other complex nucleations, oligomerization, and polymerization, which lastly produce a new amorphous three-dimensional network structure with a novel aluminosilicate-based polymer as shown in Figure 1, the figure is adapted from [55].

The alkaline liquids in geopolymer concrete are sodium hydroxide or potassium hydroxide mixed with sodium silicate or potassium silicate and water. Alkaline solutions are concentrated aqueous alkali hydroxide or silicate solutions containing soluble alkali metals, mainly sodium or potassium-based, used in the manufacturing of alkali activators for balancing the negative charge of the alumina if fourfold cooperation with the silica is achieved [2]. The purity of sodium hydroxide is around 97% and the two major states of sodium hydroxide are pellets and flakes. Meanwhile, the composition of sodium silicate

consists of three main compounds, namely SiO_2 , Na_2O , and H_2O . Regarding the reviewed papers, the range of SiO_2 was between 28 and 37 percent, Na_2O was between 8 and 18 percent, and the proportion of H_2O was between 45 and 64 percent, as shown in Table 2. These solutions generated a geopolymeric binder by activating and extracting Si and Al elements from the different source binder materials, as stated by Ouyang et al. [56].

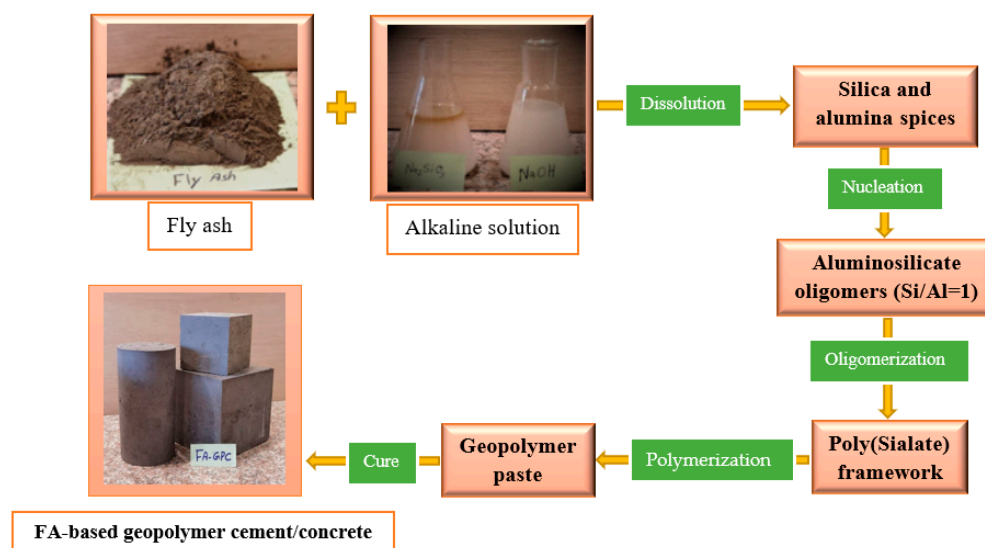


Figure 1. The schematic graphical representation shows the transition of fly ash to fly ash-based geopolymer cement/concrete.

Several research studies have been published in the literature to highlight the effect of various parameters on the fresh, physical, mechanical, durability, and microstructural properties of FA-BGPC. The compressive strength (σ_c) is one of the essential mechanical characteristics of concrete structures, and it usually provides a general performance regarding the quality of the concrete [57]. The σ_c test is carried out by following the standard test method of ASTM C39 [58]. The former paper [19] aimed to provide and develop some empirical equations among mechanical properties of different source binder materials-based geopolymer concrete. It was found that there is a lack of a systematic and comprehensive review on the impact of a wide range of mixed proportion parameters and curing conditions on the σ_c of FA-BGPC from an early age to older curing ages and different curing temperatures. As a consequence, in this study, the influence of several parameters such as the ratio of SiO_2 to Al_2O_3 of the fly ash, alkaline liquid to the binder ratio, superplasticizers and extra water content, fly ash content, fine and coarse aggregate content, sodium hydroxide and sodium silicate content, the ratio of sodium silicate to sodium hydroxide, molarity, curing temperature, curing duration inside ovens, and specimens ages on the σ_c of FA-BGPC was investigated using 800 samples from the literature studies.

Table 1. Chemical composition of fly ash.

| References | Sp. Gr. | SiO_2 | Al_2O_3 | Fe_2O_3 | CaO | MgO | K_2O | Na_2O | SO_3 | LOI |
|------------|---------|----------------|-------------------------|-------------------------|--------------|--------------|----------------------|-----------------------|---------------|------|
| [59] | - | 53.3 | 26.49 | 10.86 | 1.34 | 0.77 | 0.8 | 0.37 | 1.7 | 1.39 |
| [60] | - | 77.1 | 17.71 | 1.21 | 0.62 | 0.9 | - | 0.8 | 2.2 | 0.87 |
| | - | 62.9 | 25.8 | 3.1 | 2.3 | 0.3 | - | - | - | 1.7 |
| | - | 66.6 | 25.9 | 0.9 | 0.4 | 0.1 | - | - | - | 1.3 |
| [61] | - | 77.2 | 15.2 | 2.5 | 0.6 | 0.3 | - | - | - | 0.7 |
| | - | 43.4 | 26.2 | 17.4 | 5.4 | 1.4 | - | - | - | 0.7 |
| | - | 52.7 | 33.4 | 9 | 1 | 0.6 | - | - | - | 0.4 |

Table 1. Cont.

| References | Sp. Gr. | SiO ₂ | Al ₂ O ₃ | Fe ₂ O ₃ | CaO | MgO | K ₂ O | Na ₂ O | SO ₃ | LOI |
|------------|---------|------------------|--------------------------------|--------------------------------|-------|------|------------------|-------------------|-----------------|-------|
| [62] | 1.95 | 62.5 | 29.02 | 4.22 | 1.1 | - | - | 0.2 | 0.22 | 0.52 |
| [63] | - | 62.1 | 25.5 | 4.28 | 3.96 | 1.27 | - | - | 0.73 | - |
| [64] | 1.95 | 62.5 | 29.02 | 4.22 | 1.1 | - | - | 0.2 | 0.22 | 0.52 |
| [65] | 2.13 | 57.9 | 31.1 | 5.07 | 1.29 | 0.97 | 1 | 0.09 | 0.05 | 0.8 |
| [66] | 2.42 | 65.6 | 26.5 | 5.49 | 0.31 | 0.76 | 0.23 | 0.36 | 0.31 | 0.41 |
| [67] | 2.12 | 70.3 | 23.1 | 1.4 | 0.2 | 0.6 | 0.9 | 0.4 | 0.2 | 2 |
| [68] | - | 47.8 | 24.4 | 17.4 | 2.42 | 1.19 | 0.55 | 0.31 | 0.29 | 1.1 |
| [69] | 2.2 | 62.3 | 28.1 | 2.1 | 0.5 | 1 | 1 | 0.5 | 0.4 | 2.5 |
| [70] | - | 52 | 33.9 | 4 | 1.2 | 0.81 | 0.83 | 0.27 | 0.28 | 6.23 |
| [71] | - | 49 | 31 | 3 | 5 | 3 | 1 | 4 | 0 | 0 |
| [72] | - | 48 | 29 | 12.7 | 1.76 | 0.89 | 0.55 | 0.39 | 0.5 | 1.61 |
| [73] | - | 32.1 | 19.9 | 16.91 | 18.75 | 3.47 | 2.38 | 0.69 | 2.24 | 0.07 |
| [74] | - | 51.5 | 23.63 | 15.3 | 1.74 | 1.2 | 0.84 | 0.38 | 0.28 | 1.78 |
| [75] | 2.04 | 59.2 | 24.36 | 7.074 | 2.235 | 1.4 | 3.37 | 0.378 | - | 1.517 |
| | 2.3 | 62.3 | 21.14 | 7.347 | 1.568 | 2.35 | 0.73 | 2.445 | - | 2.071 |
| [76] | 2.05 | 64.9 | 26.64 | 5.69 | 0.33 | 0.85 | 0.25 | 0.49 | 0.33 | 0.45 |
| [77] | - | 47.8 | 24.4 | 17.4 | 2.42 | 1.19 | 0.55 | 0.31 | 0.29 | 1.1 |
| [78] | - | 59.7 | 28.36 | 4.57 | 2.1 | 0.83 | - | 0.04 | 0.4 | 1.06 |
| [79] | 2.36 | 37.6 | 14.79 | 18.56 | 19.61 | 2.7 | 0.98 | 0.73 | 4.81 | - |
| [80] | - | 53.7 | 27.2 | 11.17 | 11.17 | 1.9 | 0.54 | 0.36 | 0.3 | 0.68 |
| [81] | 2.54 | 42.4 | 21.3 | 15.7 | 13.2 | 2.3 | 2 | 0.9 | 1 | 0.4 |
| [82] | - | 50.7 | 28.8 | 8.8 | 2.38 | 1.39 | 2.4 | 0.84 | 0.3 | 3.79 |
| [83] | - | 50.7 | 28.8 | 8.8 | 2.38 | 1.39 | 2.4 | 0.84 | 0.3 | 3.79 |
| [84] | - | 50.5 | 26.57 | 13.77 | 2.13 | 1.54 | 0.77 | 0.45 | 0.41 | 0.6 |

Table 2. Purity of sodium hydroxide and compositions of sodium silicate.

| References | Sodium Hydroxide | Sodium Silicate | | |
|------------|------------------|------------------|-------------------|-------|
| | Purity% | SiO ₂ | Na ₂ O | Water |
| [59] | 98 | 29.4 | 14.7 | 55.9 |
| [60] | 97 | 34.31 | 16.37 | 49.28 |
| [61] | 98 | 29.4 | 14.7 | 55.9 |
| [63] | 98 | 32.4 | 13.7 | 53.9 |
| [65] | 98 | 34.64 | 16.27 | 49.09 |
| [66] | 98 | 35.06 | 16.95 | 47.99 |
| [68] | 98 | 29.4 | 14.7 | 55.9 |
| [70] | 99 | 28 | 8 | 64 |
| [76] | 99 | 45 | 55 | |
| [77] | 98 | 29.4 | 14.7 | 55.9 |
| [78] | 98 | 34.64 | 16.27 | 49.09 |
| [79] | 99 | 34.72 | 16.2 | 49.08 |
| [80] | 98.5 | 30.1 | 11.4 | 58.6 |
| [85] | 97 | 36.7 | 18.3 | 45 |
| [86] | 98 | 29.93 | 12.65 | 56.42 |
| [87] | 99 | 29.4 | 14.7 | 55.9 |
| [88] | 99.51 | 28 | 9 | 63 |

2. Research Significance

The primary goal of this research is to look at the impact of various mixture proportions and curing regimes on the σ_c of FA-BGPC. Despite the widespread use of geopolymer concrete, according to the authors of this study's extensive review on the subject, there is no comprehensive systematic review that shows the impact of different mixture proportions and curing regimes on the σ_c behavior of FA-BGPC. As a result, the effect of several parameters such as fly ash SiO₂/Al₂O₃ (Si/Al), alkaline liquid to binder ratio (l/b), superplasticizers and extra water content, fly ash (FA) content, fine aggregate (F) content, coarse aggregate (C) content, sodium hydroxide (SH) content, sodium silicate (SS) content,

SS/SH, molarity (M), curing temperature (T), and curing duration inside ovens (CD) were quantified. Thus, approximately 800 tested specimens with different Si/Al, l/b, FA, F, C, SH, SS, SS/SH, M, T, and CD were collected and analyzed to broaden the horizons of researchers and the construction industry by providing significant information about the influence of these different parameters on the σ_c of FA-BGPC.

3. Methodology

During the preparation of the database, an extensive literature search was made using the different search engines of several databases such as Google Scholar, Scopus, Web of Science, and ScienceDirect.

A wealth of information is available in the literature about geopolymer concrete with various source binder materials such as FA, GGBFS, RHA, SF, MK, RM, etc. However, the authors of this study focused on those studies that used FA as a source binder material to make geopolymer concrete composites. In this study, an extensive search was made to collect a relatively large amount of tested data (800 datasets) for the properties of the compressive strength of fly ash-based geopolymer concrete composites.

The datasets were made up of the Si/Al ranges from 0.48–7.7, the l/b ranges from 0.25–0.92, the FA ranges from 254–670 kg/m³, the F ranges from 318–1196 kg/m³, the C ranges from 394–1591 kg/m³, the SH ranges from 25–135 kg/m³, the SS ranges from 48–342 kg/m³, the SS/SH ranges from 0.4–8.8, the M ranges from 3–20, the T ranges from 23–120 °C, and the CD ranges from 8–168 h, as depicted in Table 3. The datasets were then utilized to study the impact of these parameters on the σ_c of fly ash-based geopolymer concrete composites. Further details of the data collection and reviewing work are summarized in a flow chart in Figure 2.

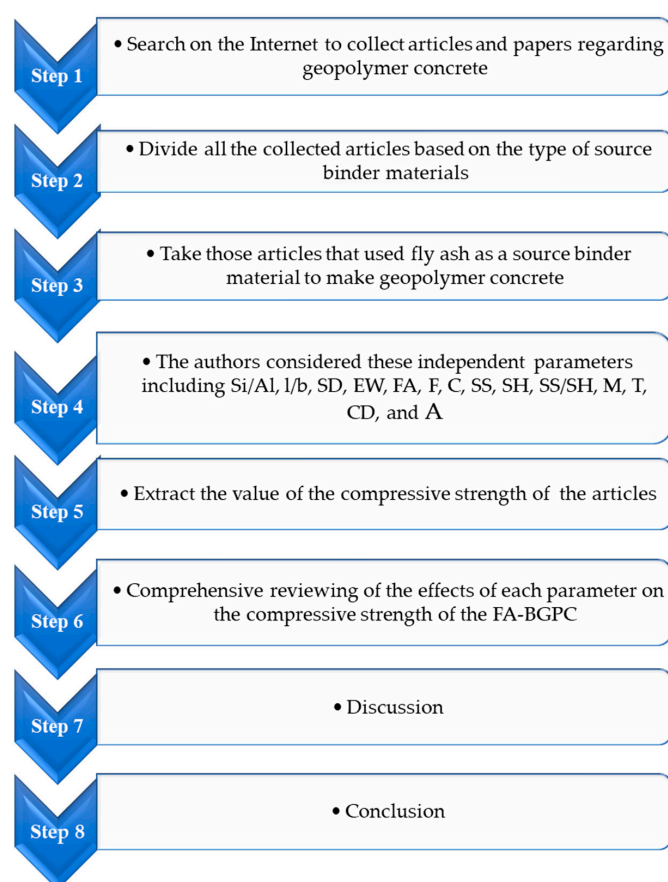


Figure 2. The flow chart diagram process followed in this study.

Table 3. Summary of different fly ash-based geopolymer concrete mixes.

| References | (Si/Al) | (I/b) | FA (kg/m ³) | F (kg/m ³) | C (kg/m ³) | SH (kg/m ³) | SS (kg/m ³) | (SS/SH) | M | T (°C) | CD (hr.) | A (Day) | fc' (MPa) |
|------------|---------|-----------|-------------------------|------------------------|------------------------|-------------------------|-------------------------|---------|-------|--------|----------|---------|-----------|
| [59] | 2 | 0.35 | 476 | 554 | 1294 | 48–120 | 48–120 | 0.4–2.5 | 8–14 | 24–90 | 8–96 | 3–94 | 17–64 |
| [60] | 1.5–5.1 | 0.5–0.6 | 300–500 | 471–664 | 1000–1411 | 42–120 | 90–215 | 1.5–2 | 12–16 | 70 | 24 | 7 | 16–64 |
| [61] | 2.4 | 0.6 | 385 | 601.7 | 1203 | 66 | 165 | 2.5 | 12 | 80 | 24 | 3–28 | 74–81 |
| [62] | 2.1 | 0.45 | 350–400 | 505–533 | 1178–1243 | 45–52 | 112–129 | 2.5 | 8–16 | 24 | - | 3–28 | 7–41 |
| [63] | 1.8 | 0.45–0.55 | 300–350 | 698–753 | 1048–1131 | 38–55 | 96–118 | 2.5 | 10 | 100 | 24 | 7–28 | 26–36 |
| [64] | 2.4 | 0.45 | 298–430 | 533–590 | 1243–1377 | 38–55 | 96–138 | 2.5 | 8–14 | 10–90 | 24 | 3–28 | 19–43 |
| [65] | 3.0 | 0.81 | 409 | 686 | 909 | 129 | 204 | 1.58 | 15 | 80 | 24 | 28–96 | 22–27 |
| [66] | 2.3 | 0.35–0.5 | 327–409 | 554–672 | 1201–1294 | 40–54 | 108–112 | 2–2.5 | 8–16 | 60 | 24 | 28 | 31–62 |
| [67] | 1.9 | 0.35 | 408 | 554 | 1294 | 41 | 103 | 2.5 | 8–14 | 60 | 24 | 7 | 40–64 |
| [68] | 2.2 | 0.3–0.45 | 400 | 830–895 | 830–895 | 32–52 | 85–129 | 2–3.3 | 12–18 | 50 | 48 | 7–28 | 16.36 |
| [69] | 1.5 | 0.3–0.5 | 400–475 | 529–547 | 1235–1280 | 34–57 | 85–142 | 2.5 | 14 | 24 | - | 7–56 | 7–44 |
| [70] | 1.6 | 0.35 | 408 | 647 | 1202 | 41 | 103 | 2.5 | 14 | 24–60 | 24 | 28 | 27–40 |
| [71] | 1.6 | 0.6 | 390 | 585 | 1092 | 67 | 167 | 2.5 | 8–18 | 24 | - | 28 | 23–32 |
| [72] | 2.1 | 0.35–0.38 | 408 | 660 | 1168–1201 | 41 | 103 | 2.5 | 10–16 | 24–50 | 24 | 28 | 25–72 |
| [73] | 2.8 | 0.55 | 356 | 554.4 | 1293 | 43–78 | 117–152 | 1.5–3.5 | 10 | 60 | 48 | 7–28 | 23–35 |
| [74] | 2.4–2.9 | 0.45 | 500 | 575 | 1150 | 64 | 160 | 2.5 | 14 | 24 | - | 28 | 44–52 |
| [75] | 0.4 | 0.4 | 350 | 650 | 1250 | 41 | 103 | 2.5 | 8 | 24–60 | 24 | 3–28 | 6–32 |
| [76] | 1.9 | 0.35 | 408 | 640–647 | 1190–1202 | 41 | 103 | 2.5 | 14–16 | 60 | 24 | 28 | 42–62 |
| [77] | 1.9 | 0.3 | 670 | 600 | 970 | 80 | 120 | 1.5 | 3–9 | 50 | 72 | 3–7 | 59–61 |
| [78] | 1.9 | 0.6 | 450 | 500 | 1150 | 135 | 135 | 1 | 10 | 40 | 24 | 7–96 | 18–49 |
| [79] | 1.7 | 0.4 | 400 | 554 | 1293 | 45 | 113 | 2.5 | 14 | 100 | 72 | 3–28 | 29–45 |
| [80] | 1.7 | 0.4 | 400 | 554 | 1293 | 45 | 113 | 2.5 | 14 | 100 | 72 | 3–28 | 29–45 |
| [81] | 1.9 | 0.37–0.4 | 408 | 647 | 1201 | 62–68 | 93–103 | 1.5 | 14 | 60 | 24 | 28 | 32–38 |
| [82] | 2.3–3.3 | 0.4 | 420–440 | 340–575 | 660–1127 | 60–68 | 150–169 | 2.5 | 12 | 80–120 | 72 | 7 | 21–61 |
| [83] | 1.9 | 0.35 | 356–444 | 554–647 | 1170–1248 | 36–44 | 89–111 | 2.5 | 14 | 60 | 24 | 7–28 | 24–63 |
| [84] | 3 | 0.35 | 409 | 549 | 1290 | 41 | 102 | 2.5 | 10 | 24 | - | 7–112 | 10–41 |
| [85] | 2.1 | 0.38–0.46 | 350–400 | 540–575 | 1265–1343 | 38–53 | 95–132 | 2.5 | 16 | 24–90 | 24 | 3–28 | 2.6–44 |
| [86] | 1.5 | 0.35 | 408 | 554 | 1294 | 41 | 103 | 2.5 | 8 | 24 | - | 7–28 | 12–16 |
| [87] | 2.1 | 0.35–0.65 | 254–420 | 318–1198 | 394–1591 | 25–76 | 69–165 | 1.5–3.5 | 8–16 | 24–120 | 6–72 | 3–28 | 13–60 |
| [88] | 1.9 | 0.4 | 400 | 651 | 1209 | 45 | 114 | 2.5 | 14 | 24 | - | 3–96 | 5–33 |
| [89] | 2.4 | 0.4 | 440 | 723 | 1085 | 64 | 112 | 1.75 | 12 | 60 | 48 | 3–28 | 23–35 |
| [90] | 1.5–3.9 | 0.7–0.9 | 412–420 | 693–706 | 918–936 | 39–92 | 241–342 | 2.6–8.8 | 15 | 80 | 24 | 3–96 | 22–57 |
| [91] | 2.5 | 0.55 | 310 | 649 | 1204 | 48.8 | 122 | 2.5 | 10 | 80 | 24 | 28–96 | 44–47 |
| [92] | 2.6–2.9 | 0.5 | 420 | 630 | 1090 | 60 | 150 | 2.5 | 12 | 80 | 24 | 7 | 32–41 |
| [93] | 1.5 | 0.37 | 424 | 598 | 1169–1197 | 63 | 95 | 1.5 | 14 | 70 | 24 | 3–96 | 2–58 |
| [94] | 2.3 | 0.5 | 368 | 554 | 1293 | 52 | 131 | 2.5 | 16 | 100 | 24 | 28 | 41 |
| [95] | 2.1–2.6 | 0.3 | 450 | 788–972 | 945–972 | 67 | 67 | 1 | 10 | 70 | 24 | 7–28 | 25–41 |
| [96] | 5.6 | 0.4 | 410 | 530 | 1044 | 67 | 117 | 1.74 | 10 | 24–75 | 26 | 7–180 | 4–36 |
| [97] | 2.3 | 0.45 | 500 | 550 | 1100 | 64.3 | 160.7 | 2.5 | 14 | 70 | 48 | 28 | 49.5 |
| [98] | 1.9 | 0.4 | 400 | 651–656 | 1209–1218 | 40–46 | 100–114 | 2.5 | 14 | 24 | - | 28–90 | 25–41 |
| [99] | 1.6 | 0.58 | 380 | 462 | 1386 | 62 | 156 | 2.5 | 10 | 60 | 24 | 28–56 | 18–23 |

Table 3. Cont.

| References | (Si/Al) | (l/b) | FA (kg/m ³) | F (kg/m ³) | C (kg/m ³) | SH (kg/m ³) | SS (kg/m ³) | (SS/SH) | M | T (°C) | CD (hr.) | A (Day) | fc' (MPa) |
|----------------------------------------------|---------|-----------|----------------------------|------------------------|------------------------|----------------------------|----------------------------|---------|-------|--------|----------|---------|-----------|
| [100] | 2.2 | 0.5 | 414 | 588 | 1091 | 69–104 | 104–138 | 1–2 | 10–20 | 24–60 | 24 | 7–28 | 19–54 |
| [101] | 1.9 | 0.4 | 394 | 554 | 1293 | 45 | 112 | 2.5 | 12 | 24–60 | 24 | 7–28 | 8–28 |
| [102] | 2.1 | 0.3–0.4 | 428 | 630 | 1170 | 44–57 | 114–122 | 2–2.5 | 8–14 | 60–90 | 24 | 3–7 | 20–49 |
| [103] | 1.5 | 0.3 | 563 | 732 | 5994 | 44 | 124 | 2.8 | 10 | 75 | 16 | 28 | 33–45 |
| [104] | 3.1 | 0.5 | 400 | 650 | 1206 | 50–70 | 140–154 | 2–2.75 | 14 | 60 | 168 | 7–28 | 30–36 |
| [105] | 7.7 | 0.4–0.6 | 345–394 | 554 | 1294 | 45–83 | 94–148 | 1.5–2.5 | 8–16 | 24 | - | 28 | 7–22 |
| [106] | 2.0 | 0.4 | 400 | 644 | 1197 | 53 | 107 | 2 | 10 | 24 | - | 3–56 | 5–23 |
| [107] | 1.8 | 0.4 | 394 | 554 | 1293 | 45 | 112 | 2.5 | 8 | 24 | - | 7–28 | 3–18 |
| [108] | 1.8 | 0.4 | 350 | 483 | 1081 | 40 | 100 | 2.5 | 14 | 24 | - | 7–28 | 3–23 |
| [109] | 1.7 | 0.45 | 436 | 654 | 1308 | 56 | 140 | 2.5 | 8 | 24 | - | 3–12 | 8–18 |
| [110] | 2.7 | 0.45 | 380 | 660 | 1189 | 48 | 122 | 2.5 | 8 | 24 | - | 28 | 30 |
| [111] | 2.6 | 0.65 | 639 | 639 | 959 | 121 | 304 | 2.5 | 8–12 | 24 | - | 7–28 | 6–32 |
| [112] | 1.6 | 0.35 | 500 | 623 | 1016 | 70 | 105 | 1.5 | 14–16 | 24 | - | 3–28 | 7–27 |
| [113] | 2.1 | 0.41 | 350 | 645 | 1200 | 41 | 103 | 2.5 | 8 | 24 | - | 3–56 | 7–21 |
| [114] | 2.3 | 0.4 | 394 | 646 | 1201 | 45 | 112 | 2.5 | 16 | 24–60 | 24 | 3–28 | 8–50 |
| Remarks (Ranges are varied between) | 0.4–7.7 | 0.25–0.92 | 254–670 | 318–1196 | 394–1591 | 25–135 | 48–342 | 0.4–8.8 | 3–20 | 23–120 | 8–168 | 3–112 | 2–64 |

4. Mixture Proportion Parameters

4.1. Chemical Composition of Fly Ash ($\text{SiO}_2/\text{Al}_2\text{O}_3$) (Si/Al)

Various fly ashes with slightly different chemical compositions, specific surfaces, and specific gravity were used in the literature to prepare the geopolymer concrete. Based on ASTM C618 [29], ash with a summation of their $\text{SiO}_2 + \text{Al}_2\text{O}_3 + \text{Fe}_2\text{O}_3$ greater than 70% can be known as fly ash. The Si/Al ratio of the fly ashes ranged from 0.48 to 7.7, with an average of 2.58, the variance of 2.06, the standard deviation of 1.44, skewness of 2.83, and kurtosis of 7.31 based on 800 data points obtained from several research works. In a symmetrical normal distribution, skewness refers to distortion or asymmetry. When the curve in a dataset is shifted to the right or left, it is said to be skewed. For example, the skew of zero was measured for a normal distribution and the right skew was measured as an indication of lognormal distribution [115].

An experimental laboratory research work was conducted by Thakur and Ghosh [116] to investigate the effect of silica content on the σ_c and microstructure of FA-BGPC. They reported that the σ_c was improved almost linearly with Si content up to 4, and then it was decreased, as illustrated in Figure 3, the figure is adapted from [116].

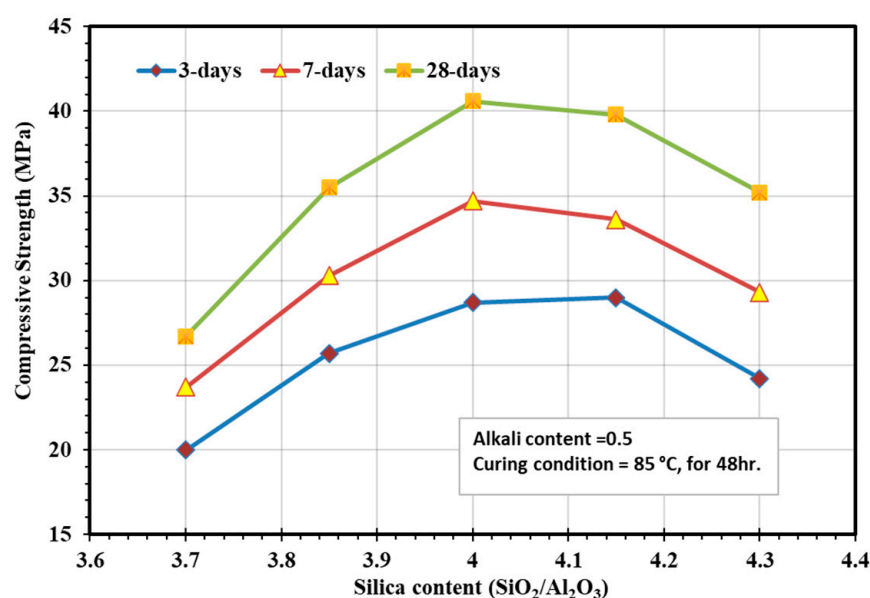


Figure 3. Effect of different $\text{SiO}_2/\text{Al}_2\text{O}_3$ on the σ_c of FA-BGPC.

In the same context, a research study was carried out on the FA-BGPC by Al-Azzawi et al. [60] who used five different types of fly ashes. The fly ashes had different chemical compositions with the ratio of Si/Al of 1.58, 1.66, 2.44, 2.57, and 5.08. The highest σ_c was recorded for the fly ash with a Si/Al ratio of 1.66, which was 34 MPa. This value was significantly higher than the other fly ash geopolymer concrete specimens by 20.5%, 38.2%, 41.2%, and 44.1% for the Si/Al of 1.58, 2.44, 2.57, and 5.08, respectively. This result could be explained by the fact that varied fly ash characteristics lead to varying degrees of polymerization between the alkaline activator and the fly ashes, which influences the σ_c of the geopolymer concrete. Furthermore, the degree to which the polymerization process is carried out has an impact on the microstructure of the FA-BGPC, which in turn reflects on the σ_c of the geopolymer concrete [60].

Moreover, an experimental investigation was carried out to demonstrate the impact of two distinct types of fly ash on the mechanical and durability qualities of FA-BGPC. At 28 days, the compression strength was 51.6 and 44.8 MPa at ambient curing temperature for Si/Al ratios of 2.43 and 2.95, respectively [74]. The fly ash's reduced CaO content and low activity were blamed for this finding [117,118]. Furthermore, to investigate the long-term permeation characteristics of the geopolymer concrete, four different types of

fly ashes were used to prepare FA-BGPC. Their results claimed that the highest σ_c was achieved for the geopolymer concrete with a Si/Al of 1.71, and the lowest σ_c was recorded at a Si/Al of 1.8, while the other fly ash types fell between the two. Moreover, all their geopolymer concrete mixtures archived almost 70% of their one-year σ_c at three days. For instance, the geopolymer concrete with a Si/Al of 1.71 displayed about a 20 MPa strength increment between 3 and 365 days [90]. This result revealed a continuous improvement in the polymerization process, which leads to progress in the σ_c of different types of FA-BGPC. This output contrasts with past studies on FA-BGPC, which recorded a slight subsequent improvement in the σ_c for the heat curing conditions [59,119,120]. In the same manner, another research study was carried out on the mechanical characteristics of geopolymer concrete. They used three different fly ashes with different chemical compositions. In the controlled heat curing conditions and constant mixture proportions, the σ_c values were 32.1, 41, and 36.6 MPa for the Si/Al of the fly ash of 2.9, 2.78, and 2.6, respectively [92]. The results behind different σ_c values were examined by Scanning electron microscopy (SEM). They reported that the samples made from the fly ash with a Si/Al of 2.78 had the highest degree of reacted fly ash spheres participating in the greatest σ_c . This result was reported by other researchers who claimed that the total reacted Si/Al is crucial to the progress in the polymerization of FA-BGPC [59,119]. Similarly, the σ_c of geopolymer concrete improved as the Si/Al ratio was raised [69,121,122].

For example, Thokchom et al. [122] discovered that increasing the Si/Al ratio of the source binder materials enhanced residual σ_c of the geopolymer concrete when the specimens were exposed to various temperatures, as shown in Figure 4, the figure is adapted from [122]. The geopolymer concrete with a 2.2 ratio of Si/Al preserved nearly 63% of its σ_c even after exposure to 900 °C, while the geopolymer concrete mixture with a 1.7 ratio of Si/Al had a residual σ_c of 50%. SEM examinations confirmed that the geopolymer concrete specimens prepared with a Si/Al ratio of 1.7 had complete matrix disruption due to phase sintering inside the samples but that the interconnected matrix had most of the original pores sealed during the heating process. Geopolymer concrete with a Si/Al ratio of 2.2, on the other hand, has a generally undisturbed matrix except in a few locations [122].

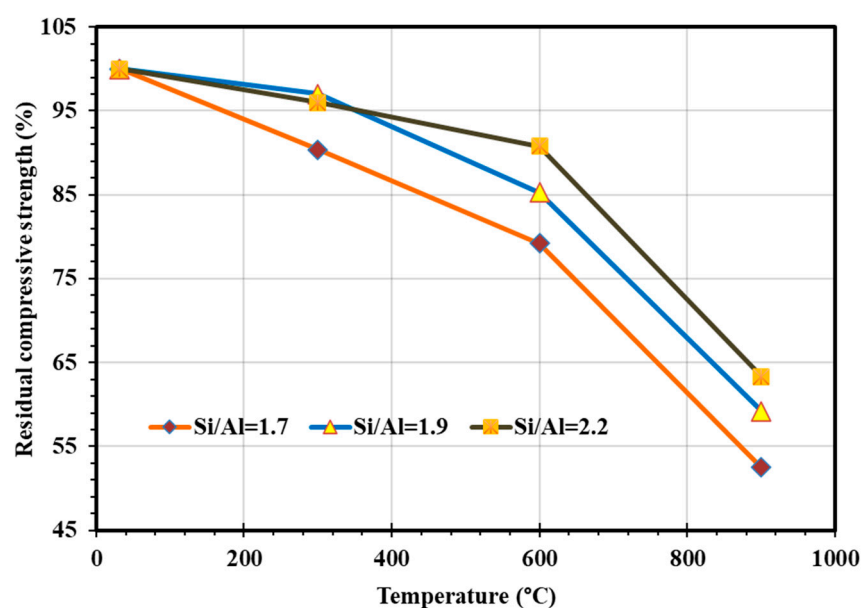


Figure 4. Variation of residual σ_c of different Si/Al ratios of FA-BGPC with temperature.

Finally, mechanical properties of high early strength FA-BGPC were investigated using an experimental study program. They used five types of fly ash as a source binder, each with a different Si/Al ratio and CaO content. Their results indicated that the mixture with

2.18 Si/Al and 4.96 CaO content had the highest σ_c [95]. Figure 5 which is adapted from [95] shows the variation of σ_c of FA-BGPC with different percentages of CaO and $\text{SiO}_2 + \text{Al}_2\text{O}_3$ of fly ash, emphasizing the idea that the CaO, SiO_2 , and Al_2O_3 content has a direct impact on the mechanical properties of FA-BGPC. The high CaO fly ash-based geopolymer concrete mixture gains strength due to two main distinct mechanisms, namely polymerization and hydration under-regulated curing conditions, which can explain this outcome. The σ_c of the FA-BGPC increased as the SiO_2 and Al_2O_3 content of the fly ash increased due to the polymerization process, while the lack of CaO inhibits the polymerization process, the σ_c of geopolymer concrete suffers as a result [123].

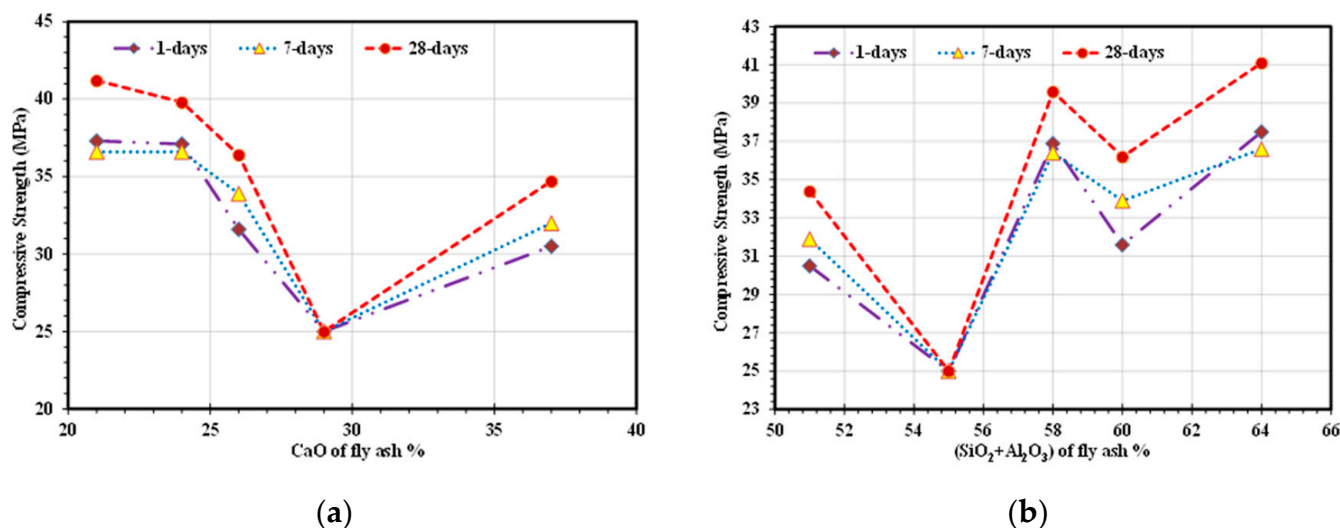


Figure 5. Variation of σ_c of FA-BGPC versus (a) calcium content and (b) silica and alumina contents.

4.2. Alkaline Solution to the Binder Ratio (l/b)

The term “alkaline solution” refers to the sum of the sodium hydroxide and sodium silicate contents, whereas “binder content” refers to the entire weight or volume of fly ash or other source binder materials in the geopolymer concrete’s mixed proportions [19,54]. Based on the collected data from the literature studies, the l/b ratio of the FA-BGPC varied between 0.25 and 0.92, with an average variance, standard deviation, skewness, and kurtosis of 0.46, 0.01, 0.1, 1.24, and 2.31, respectively. The variance is a measure of variability that is calculated by averaging the squared deviations from the mean. Additionally, variance indicates the degree of spread within the dataset. The wider the data distribution, the larger the variance in proportion to the mean [124].

Based on the findings of Aliabdo et al. [68], when the chemical admixture content, additional water content, SS/SH, and M were kept constant at 10.5 kg/m^3 , 35 kg/m^3 , 0.4, and 16, respectively, the σ_c of FA-BGPC was increased with the increment in the l/b ratio up to 0.4, and then the effect was reversed as shown in Figure 6 adapted from [68]. In comparison to a 0.3 alkaline liquid to fly ash ratio, the increase in the σ_c of FA-BGPC was 52 percent, 78 percent, and 68 percent for mixes with 0.35, 0.4, and 0.45 alkaline liquid to fly ash ratios, respectively. Similarly, Shehab et al. [63] discovered that increasing the proportion of l/b enhanced the σ_c of FA-BGPC at 7 and 28 days. In the same vein, an experiment was conducted to investigate the effect of various parameters on the mechanical properties of FA-BGPC and it was discovered that as the l/b increased up to 0.55, the σ_c was significantly increased, and beyond that, the mechanical properties of FA-BGPC were negatively affected. They reported that the σ_c of 39, 47, 58, and 44 MPa were obtained with l/b ratios of 0.35, 0.45, 0.55, and 0.65, respectively, when all other variables were constant even though different curing temperatures of 60, 80, and 100°C were used [87].

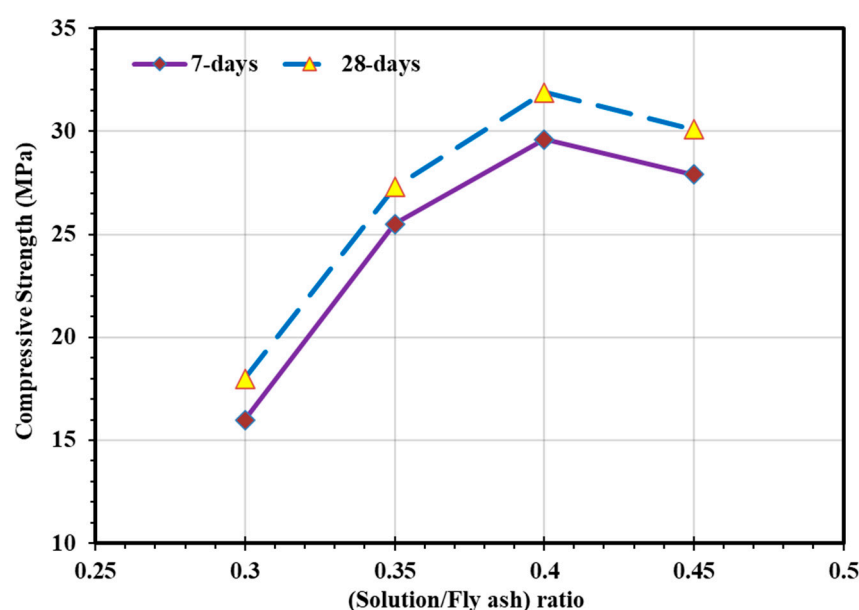


Figure 6. Effect of l/b ratios on the σ_c of FA-BGPC.

In contrast to the findings mentioned earlier, some research indicates that increasing the l/b ratio decreased the σ_c of FA-BGPC. For example, an experimental study was conducted to determine the behavior of low-CaO fly and bottom ash-based geopolymer concrete with varying l/b ratios when cured at room temperature. They observed that at 28 days, the σ_c of the geopolymer concrete was 18.8, 27.2, and 34.3 MPa, respectively, with l/b ratios of 0.5, 0.35, and 0.3 [69]. This result was attributed to the fact that the water content in the reaction medium of the geopolymer concrete mixture was increased, as any increase in the l/b ratio leads to decreased friction between the particles and, as a result, a reduction in the σ_c of the geopolymer concrete [125]. Nevertheless, only one exception to this general trend can be found in the same geopolymer concrete with an l/b ratio of 0.25, where a slight reduction in σ_c was actually observed due to a lack of workability of the geopolymer concrete mixture in the fresh state, which caused placement problems during concrete casting when compared to the other l/b ratio mixtures, and as a result, affected the σ_c value [69]. Other investigations have produced similar findings, even though each study's alkaline solution to binder ratio was different [26,66,102]. In a similar vein, Fang et al. [106] asserted that an increase in the l/b ratio substantially impacts the σ_c of blended fly ash-slag-based geopolymer concrete at early ages but has no significant impact on the compressive strength of geopolymer concrete at later ages. This finding argued that decreasing the l/b ratio will accelerate the alkaline activation process of fly ash-slag geopolymer concrete due to a decrease in the consistency of the geopolymer concrete mixture [126]. In this case, the calcium aluminate silicate hydrate (C-A-S-H) and sodium aluminate silicate hydrate (N-A-S-H) gels can be produced rapidly in a geopolymer concrete mixture with a low l/b ratio, thereby contributing to the development of the early-age σ_c of fly ash-slag geopolymer concrete [127].

Finally, it was discovered that the σ_c of lower sodium hydroxide concentrations (molarity) cured at ambient temperature declined as the l/b ratio increased. For example, for an l/b ratio of 0.4, 0.5, and 0.6, the σ_c was 11, 7.6, and 7.5 MPa, respectively, when the molarity was 8 M. The σ_c of FA-BGPC improved to 18.1, 21.5, and 21.5 MPa at 0.4, 0.5, and 0.6 l/b ratio, respectively, when the molarity was increased to 14 M [105], as shown in Figure 7, the figure is adapted from [105]. Further, increasing the l/b ratio from 0.5 to 0.6 decreases the σ_c of the geopolymer concrete by about 6.1%, 8.8%, 13.8%, 22.2%, and 14%, respectively, for sodium hydroxide concentrations of 8, 10, 12, 14, and 16 M. This finding demonstrated that raising the molarity of the alkaline liquid results in the existence of a

greater solid component relative to the water content, which has a substantial effect on the polymerization process and, as a result, compressive strength was increased [128].

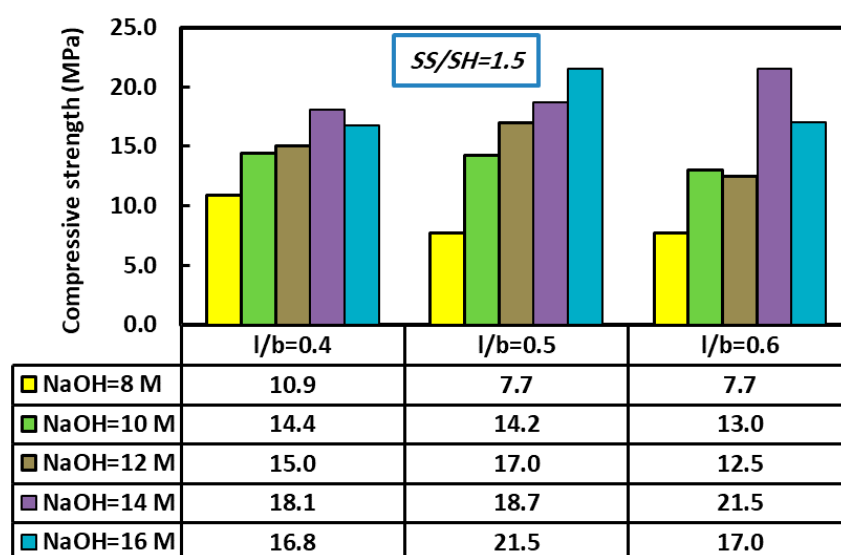


Figure 7. Effect of l/b ratios and molarity of sodium hydroxide on the σ_c of FA-BGPC with SS/SH of 1.5.

4.3. Superplasticizer Dosage and Extra Water

Superplasticizer and water content are two essential parameters that determine the workability behavior of FA-BGPC and so influence its hardened properties. Since the alkaline solution, which is composed of sodium hydroxide and sodium silicate, is more viscous than water, its use in geopolymer concrete results in a mixture that is stickier and more cohesive than conventional concrete [129]; consequently, additional water and superplasticizer are added to the geopolymer concrete mixture to improve workability.

Hardjito et al. [130] conducted an experiment to determine the influence of superplasticizer dosage on the σ_c of FA-BGPC. They used a variety of high-range water-reducing admixtures. Their findings indicated that adding superplasticizer improves the workability of the FA-BGPC on the one hand and that adding superplasticizer to the geopolymer concrete mixture has a negligible effect on σ_c up to nearly 2% fly ash by mass on the other hand, as illustrated in Figure 8, the figure is adapted from [130]. After 2% superplasticizer dosage, the σ_c declined when superplasticizer dosage was increased. For example, when the superplasticizer dosage was increased from 2% to 3.5%, the σ_c reduced by 19%. Furthermore, according to the findings of this research study [130], σ_c was dramatically reduced with the addition of excess water to the geopolymer concrete mixture at various curing temperatures. This conclusion is consistent with the findings of Barbosa et al. [131], who conducted research on geopolymer concrete pastes.

In addition, an experiment was carried out to see how the addition of more water affected the workability and σ_c of FA-BGPC. Their findings showed that increasing the amount of extra water in the geopolymer concrete mixture enhanced and improved workability while decreasing σ_c . For example, when the excess water content increased from 0.25 to 0.30, 0.35, and 0.40, the σ_c reduced by 32%, 42%, and 71%, respectively [132]. This result was attributed to the fact that water evaporates from geopolymer concrete, leaving pores and cavities within the geopolymer concrete matrix when geopolymer concrete specimens are curing at high temperatures inside ovens, and the presence of additional water may influence the alkalinity environment of the FA-BGPC matrix, thereby slowing the polymerization process [60]. In the same vein, a study was conducted to determine the effect of increased water and superplasticizer concentration on the σ_c of FA-BGPC. They concluded that as the amount of extra water in the geopolymer concrete mixture increased, σ_c decreased, as shown in Figure 9 at the ages of 7 and 28 days, this figure is

adapted from [68]. This decline in σ_c was not greater than 10% up to 30 kg/m³ of extra water but was increased to 24% when 35 kg/m³ of additional water was used [68]. They also discovered that as the superplasticizer dose increased, the σ_c of FA-BGPC reduced marginally. For example, they found that the σ_c of FA-BGPC with 5, 7.5, and 10.5 kg/m³ superplasticizer dosages were reduced by 4.2%, 8.6%, and 24%, respectively, when compared to the same mixture with 2.5 kg/m³ admixture content [68]. Furthermore, Josef and Mathew [87] found that when the water to geopolymer concrete solids ratio increased, the σ_c of FA-BGPC dropped. This reduction in σ_c is approximately linear for all values of l/b ratio, as shown in Figure 10 adapted from [87].

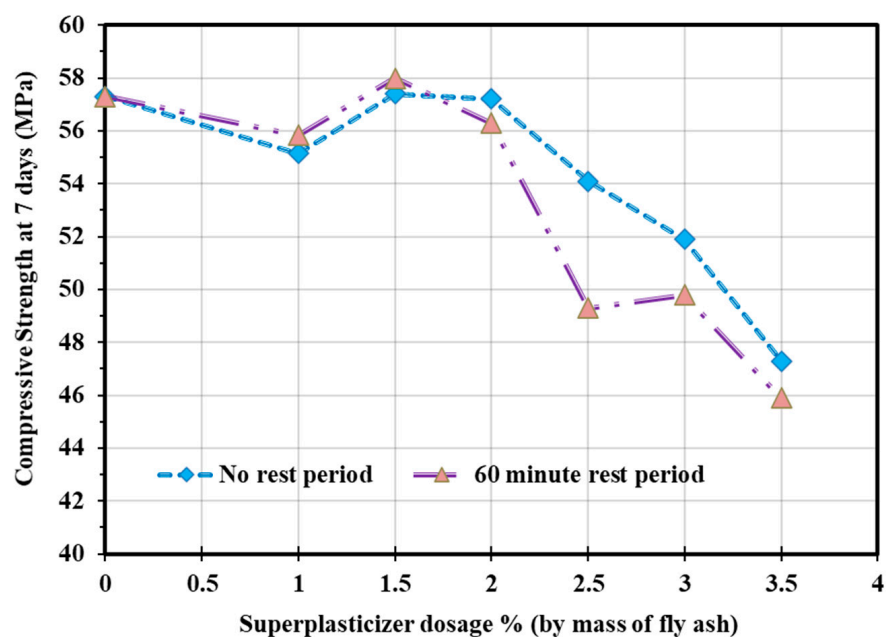


Figure 8. Effect of high-range water-reducing admixture on the σ_c of FA-BGPC.

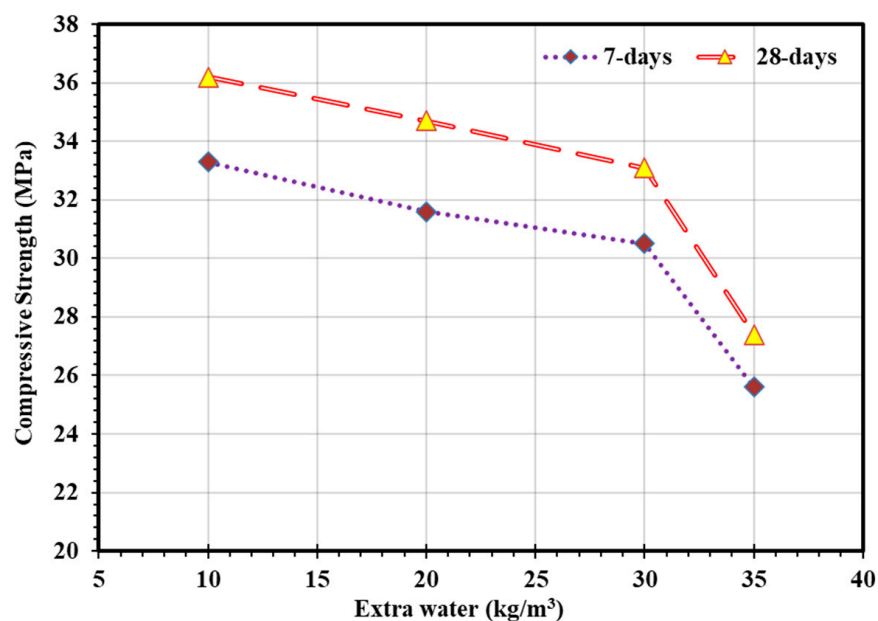


Figure 9. Effect of extra water on the σ_c of FA-BGPC.

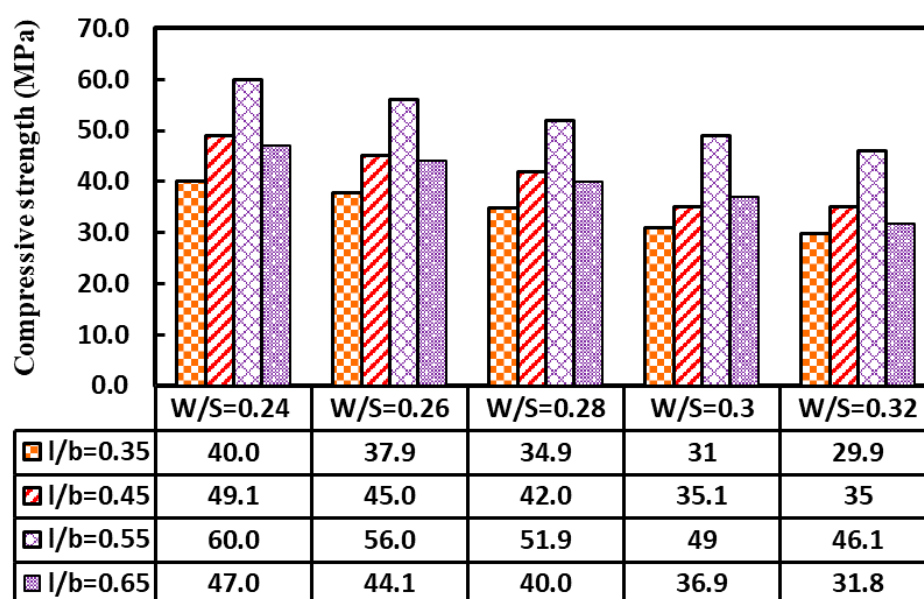


Figure 10. Effect of water to geopolymer solid on the σ_c of FA-BGPC. (Note: Total aggregate content = 70%, ratio of fine aggregate to total aggregate = 0.35, ratio of SS/SH = 2.5, curing temperature = 100 °C, and period of curing = 24 h).

Lastly, an experiment was conducted to determine the impact of superplasticizer and water to binder ratio on the σ_c of FA-BGPC. The σ_c was found to be drastically reduced as the superplasticizer dosage and water to binder ratio were increased. For instance, σ_c was reduced by 41% and 50% at 13.92 and 48 kg/m³ superplasticizer content, respectively, compared to 8.64 kg/m³ superplasticizer content; additionally, σ_c was reduced to 46.2 and 27.2 MPa at 45.6 and 60 kg/m³ extra water content, respectively, compared to 40.8 kg/m³ extra water content with the σ_c of 55.6 MPa [93]. Similar results were achieved by Vora and Dave [102], who observed that the σ_c of FA-BGPC was decreased as the superplasticizer and water to binder ratio of the concrete mixture increased. This is because the extra water in the geopolymer concrete mixture causes large gel crystals with trapped water inside. Then, once the entrapped water evaporates in the mixture, it produces a highly porous matrix, causing a decrease in σ_c and an increase in the absorption capacity of the geopolymer concrete [133]. In general, a greater proportion of water and superplasticizer in the geopolymer concrete mixture results in a decrease in the compressive strength of the geopolymer concrete composite due to decreased contact between the activating solution source reacting material [26,134].

4.4. Fly Ash (FA) Content

Due to its low cost, abundant availability, and greater potential for preparing geopolymers, fly ash (FA) is commonly employed as a source binder material for making geopolymer concrete [25,26]. For the gathered data, the content of fly ash in the mixture proportions of different Fa-BGPC ranged from 254 to 670 kg/m³. The chemical compositions of the FAs vary, and their specific gravity ranges from 1.95 to 2.54. The FA's average, standard deviation, skewness, and kurtosis were 386 kg/m³, 73.9 kg/m³, 5466, 1.52, and 4.04, respectively. The kurtosis is a statistical measure of how far the tails of a data distribution differ from the tails of a normal distribution. Kurtosis also controls the weight of the distribution tails, whereas skewness determines the symmetry of the distribution [54].

Al-Azzawi et al. [60] conducted an experimental laboratory study to investigate the effect of different fly ash contents on the bond and σ_c of FA-BGPC. They found that as the fly ash content was increased, the bond and σ_c of the geopolymer concrete improved. The maximum increase in σ_c for three different fly ash content levels for five distinct fly ash types (ER, MP, BW, GL, and CL) was 19%, 23%, 17%, 36%, and 25%, respectively, when the

fly ash content level was increased from 300 kg/m³ to 500 kg/m³ [60]. This result (based on their SEM tests) argued for the fact that higher content of fly ash in the geopolymer concrete mixture gives denser and compacted microstructure to the geopolymer concrete matrix. Additionally, the fly ash particles enhance movement among the aggregate particles due to their spherical form and smooth surface [135]; therefore, lowering the fly ash content reduces the ability of FA-BGPC components to consolidate and compact properly, lowering bond and σ_c . On the other hand, as the fly ash content increased, the volume of fine fraction particles in the geopolymer concrete matrix increased, filling the voids and pores between the aggregate particles, and hence compressive strength was improved [60]. Similar results of increased σ_c of FA-BGPC with increasing fly ash content were reported at both heat curing and ambient curing regimes [63,85]. For example, as the fly ash concentration grew from 300 to 400 kg/m³, the σ_c increased from 21 MPa to 42 MPa [85].

Furthermore, Singhal et al. [62] discovered that the σ_c of FA-BGPC improved as the fly ash content rose. For example, when the fly ash content was increased from 350 kg/m³ to 375 and 400 kg/m³, respectively, at the ambient curing age of 7 days, the σ_c improved by 11% and 32%, and increased by 15% and 24% at the age of 28 days. At the ambient curing age of 28 days, this enhancement in the σ_c of geopolymer concrete was documented for other sodium hydroxide molarities, as illustrated in Figure 11 adapted from [62]. This result can be attributed to the fact that fly ash is the primary source of aluminosilicate source materials in the geopolymer concrete mixture, and as the amount of fly ash content increased, silica and alumina levels increased, affecting polymerization reactions, resulting in increased C-A-S-H and N-A-S-H gels, and finally improved the σ_c of FA-BGPC [62].

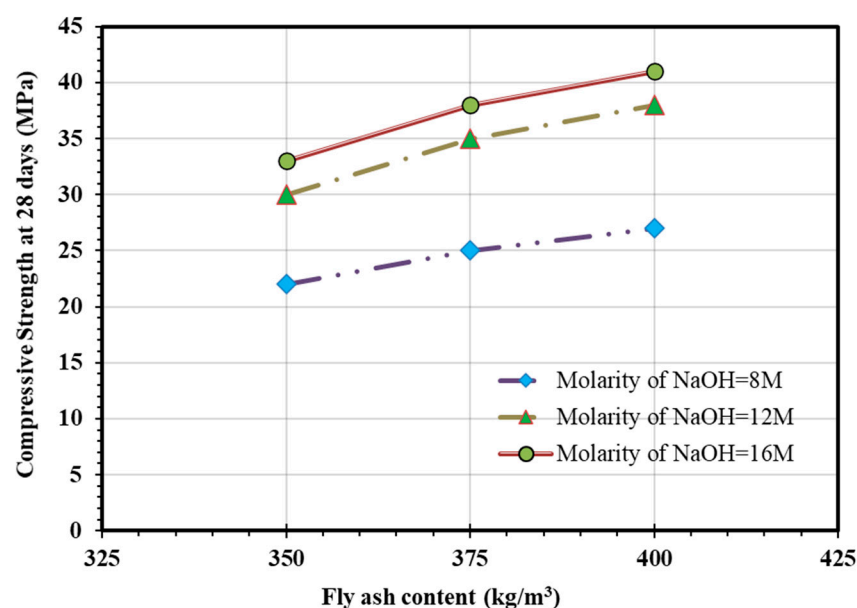


Figure 11. The σ_c of FA-BGPC with different fly ash content and molarity at ambient curing conditions.

In the same manner, a study was undertaken to evaluate the characteristics of fly ash-based geopolymer concrete. They employed varied volumes of fly ash and found that as the fly ash content grew, the σ_c of FA-BGPC increased. For example, with 356, 408, and 444 kg/m³ of fly ash concentration, the σ_c was 25.44, 36, and 48 MPa, respectively, [83]. This finding is credited to the same source as previously noted. Similarly, Ramujee and PothaRaju [66] showed that as the proportion of fly ash in the geopolymer concrete mixture increased, the σ_c increased. Overall, most studies found that the σ_c of FA-BGPC increased as the amount of fly ash in the geopolymer concrete mixture increased, implying that fly ash with a higher fineness and glassy phase is more reactive, resulting in a faster polymerization rate and, as a result, a high strength geopolymer concrete was produced [20,136,137].

4.5. Aggregate Content

The aggregates used in geopolymer concrete mixtures are the same as those used in traditional concrete mixtures, including fine and coarse particles. Previous research used the river and crushed sand with a maximum aggregate size of 4.75 mm and a specific gravity of 2.60–2.8 as fine aggregate, and its grade also met the ASTM C 33 [138] standards. For the collected 800 datasets, fine aggregate content ranged from 318 to 1196 kg/m³ for FA-BGPC mixtures, with an average of 610 kg/m³, a standard deviation of 93.8 kg/m³, a variance of 8806.7, and other statistical variables such as skewness and kurtosis were 1.49 and 5.56, respectively.

Crushed stone or gravel with a maximum aggregate size of 20 mm, on the other hand, has been employed as the coarse aggregate in the literature for the preparation of fly ash-based geopolymer concrete mixtures. The coarse aggregate content ranged from 394 to 1591 kg/m³ based on data collected from various amounts of FA-BGPC mixtures. The dataset's statistical analysis reveals that the average coarse aggregate content was 1174.5 kg/m³, the standard deviation was 148.3 kg/m³, the variance was 21,993, the skewness was −1.43, and the kurtosis was 3.0.

The influence of total aggregate content on the σ_c of FA-BGPC at various molarities and curing temperatures was investigated by Chithambaram et al. [64]. They used five different volume fractions of total aggregate contents ranging from 74% to 82%. It was discovered that the σ_c of FA-BGPC increased with the increment of entire aggregate content up to 78% and subsequently declined due to insufficient binding material for holding the aggregates together. Furthermore, as shown in Figure 12 (adapted from [64]), they observed that the highest σ_c was reached for the geopolymer concrete mixture with 78% total aggregate content at 60 °C curing conditions. However, this percentage of aggregate results in a 37.5% loss in workability compared to a geopolymer concrete mixture with 76% aggregate. As a result, they prefer to employ 76% of total aggregate content with a molarity of 12 M and cured at 90 °C since it gives a low σ_c drop (about 2.6%) without affecting the slump value of the FA-BGPC mixture [64].

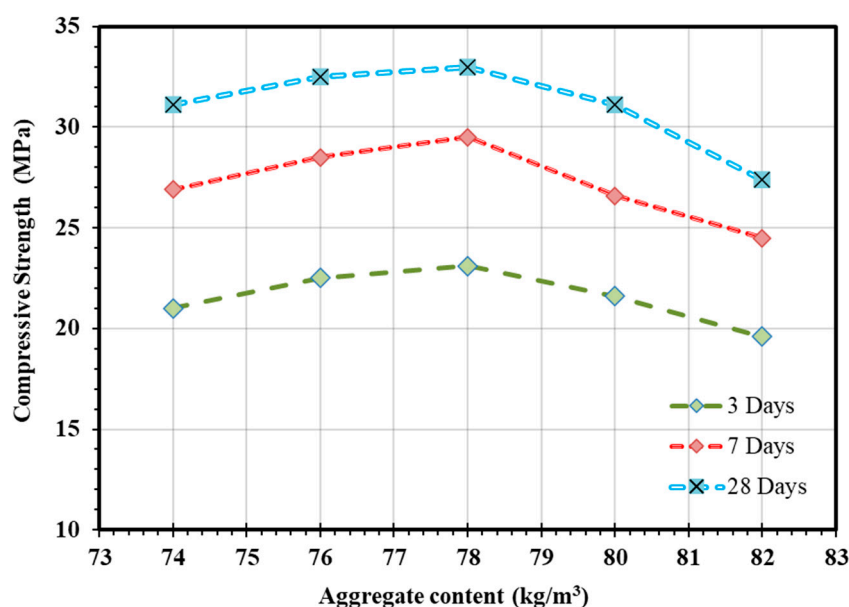


Figure 12. Effect of total aggregate content on the σ_c of FA-BGPC at the age of 3, 7, and 28 days.

In addition, an experimental study was carried out to investigate the effect of aggregate properties on the mechanical and absorption properties of fly ash-based geopolymer mortars. They employed three types of aggregates: river sand, crushed sand, and a hybrid of the river and crushed sand. They observed that the σ_c of the geopolymer mortar mixtures ranged from 28.2 to 47.8 MPa at one day when the molarity was 12 M, the SS/SH ratio

was 2.5, and the specimens were cured at 90 °C for 24 h. Moreover, when compared to other aggregates, it was discovered that the geopolymer mixture with crushed sand had a greater σ_c . This outcome was attributed to the crushed sand's rough surface texture and angular shape, which results in a higher surface-to-volume ratio and thus improved binding qualities between the aggregates and the paste matrixes [139]. Additionally, they reported that the crushed sand with a coarser grade (2–4 mm) had the maximum σ_c when compared to the other grades, as shown in Figure 13 adapted from [139]. Mane and Jadhav [140] published similar findings, stating that crushed sand had a higher σ_c than river sand. Furthermore, they observed that when granite is used as a coarse aggregate, the σ_c of the FA-BGPC is increased compared to when coarse basalt stones are used.

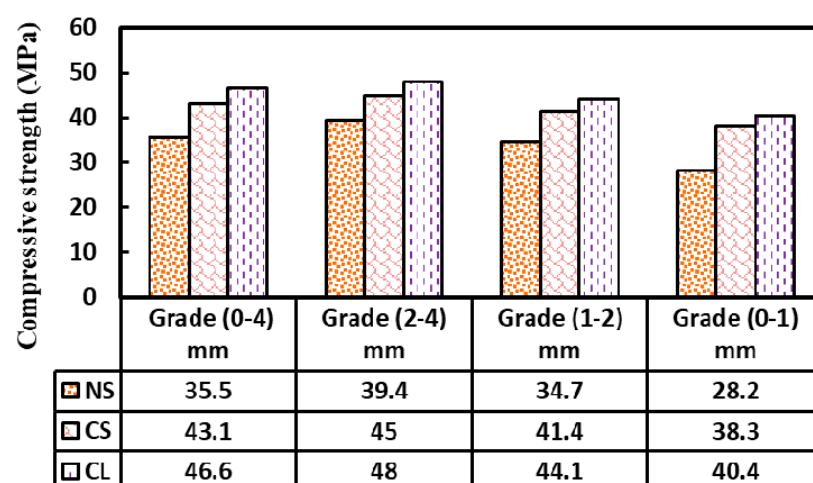


Figure 13. Effect of aggregate type and grading on the σ_c of fly ash-based geopolymer mortar at the age of 1 day. (Note: NS = natural sand, CS = combined sand, CL = crushed limestone).

In the same context, Nuaklong et al. [141] investigated the effect of recycled concrete aggregates and crushed limestone aggregates on the characteristics of FA-BGPC. They asserted that it is possible to use recycled concrete aggregates to produce FA-BGPC with a σ_c of 30–38 MPa after seven days, but this value is slightly less than that of FA-BGPC with crushed limestone aggregates, which has a σ_c of 38–41 MPa after seven days. Similar results can be obtained in other investigations, despite different mixing proportions being utilized [78].

Sreenivasulu et al. [142], on the other hand, investigated the σ_c of fly ash/GGBFS-based geopolymer concrete with varying fine aggregate contents and grades. They employed granite slurry as a natural sand replacement to create varied ratios of blended natural sand and granite slurry (100:0, 80:20, 60:40, and 40:60). In the circumstances of ambient curing conditions with the molarity of 8 M and the ratio of SS/SH of 2, they discovered that the σ_c was significantly increased in all curing ages of 7, 28, and 90 days, until the blend of 60:40 and beyond that, a decline in the σ_c was reported, as represented in Figure 14, the figure is adapted from [142]. For example, the σ_c of blended natural sand and granite slurry proportions of 60:40 was 34, 51, and 59.9 MPa for curing ages of 7, 28, and 90 days, respectively, but for the blend of 40:60, this result was 22.4, 33.6, and 38.6 MPa. These findings suggest that the granite slurry acts as a filling agent, filling the voids and pores of the geopolymer concrete and thus making the geopolymer concrete dense, resulting in an increase in σ_c of the geopolymer concrete until 40% sand replacement, after which the σ_c decreases due to the high percentages of fine materials in the geopolymer concrete mixtures [142]. Moreover, according to the findings of Embong et al. [75]. They studied the effects of replacing coarse granite aggregate with limestone. Their experiments replaced the portion of coarse granite aggregate in the geopolymer concrete mixtures with limestone 0%, 25%, 50%, 75%, and 100%. They discovered that in the ambient curing state, replacing limestone had a bigger impact on the σ_c of the FA-BGPC than in the oven curing condition.

For example, a 35.3%, 19.5%, and 14.15% increase in σ_c was attained for replacement levels of 25%, 50%, and 75%, respectively, compared to a control geopolymer concrete mixture without any limestone ingredient. This result was attributed to the formation of extra C-A-S-H gels that provided a solid structural framework in the geopolymer concrete [75]. In addition, the added solubility of Si element in fly ash to form C-A-S-H gels addresses the disadvantages of low reactivity in ambient curing circumstances [143]. However, a 10.2% decrease in σ_c was recorded for the replacement level of 100% limestone due to decreased aggregate packing density provided by evenly graded limestone in the geopolymer concrete mixtures [75]. The replacement of granite with limestone in the oven curing state, on the other hand, gives an improvement in σ_c only up to a 25% replacement level, and beyond that, a fall in σ_c was recorded, as shown in Figure 15, the figure is adapted from [75].

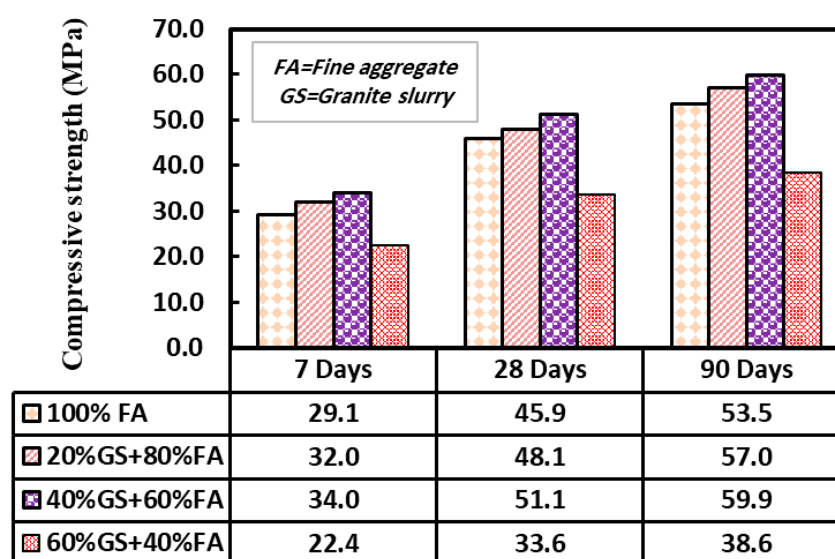


Figure 14. Effect of fine aggregate (FA) replacement by granite slurry (GS) on the σ_c of fly ash/GGBFS-based geopolymer concrete at the age of 7, 28, and 90 days.

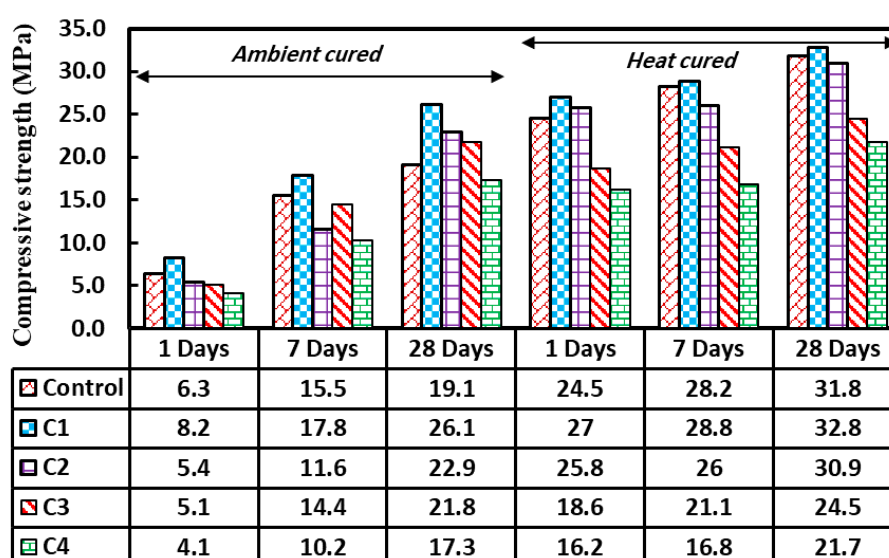


Figure 15. Effect of granite coarse aggregate replacement by limestone on the σ_c of FA-BGPC at different ages. (Note: Control = 100% Granite coarse aggregate (GA) + 0% Limestone coarse aggregate (LA), C1 = 75%GA + 25%LA, C2 = 50%GA + 50%LA, C3 = 25%GA + 75%LA, C4 = 0%GA + 100%LA).

Finally, a study was conducted to demonstrate the effect of aggregate content on the fresh and mechanical properties of FA-BGPC. They utilized various aggregate contents and fine aggregate-to-total aggregate ratios. They concluded that the σ_c of geopolymer concrete mixtures rose with increasing total aggregate content up to 70% and then decreased. Furthermore, the σ_c was increased by increasing the fine aggregate to the total aggregate ratio of 0.35 percent and subsequently reducing it [87]. As a result, a limit proportion of fine aggregate and total aggregate content for a given type of coarse and fine aggregate produced the best σ_c for the FA-BGPC.

4.6. $\text{Na}_2\text{SiO}_3/\text{NaOH}$ Ratio or SS/SH Ratio

Sodium hydroxide (NaOH) and sodium silicate (Na_2SiO_3) are commonly employed as activator solutions in preparing geopolymer concrete mixtures. The sodium hydroxide (SH) concentration of the 800 datasets gathered ranged from 25 to 135 kg/m^3 , with an average of 57 kg/m^3 , a standard deviation of 19.33 kg/m^3 , a skewness of 1.75, a kurtosis of 3.55, and a variance of 373.7. The purity of the SH in all of the FA-BGPC combinations was greater than 97 percent, with pellets and flakes being the two major states of the SH in all of the mixtures. Furthermore, the sodium silicate (SS) level was changed from 48 to 342 kg/m^3 . The SS was made up of SiO_2 , Na_2O , and water. SiO_2 levels ranged from 28 to 37%, Na_2O levels ranged from 8 to 18%, while the percentage of water in the SS ranged from 45 to 64%. The average concentration of SS in the fly ash-based geopolymer concrete mixture was 128.2 kg/m^3 , the standard deviation was 45.8 kg/m^3 , the variance was 2097, skewness was 2.56, and kurtosis was 7.73, according to the statistical analysis. Moreover, based on the data collected, the ratio of Na_2SiO_3 to NaOH varied between 0.4 and 8.8, with an average of 2.34. The standard deviation, variance, skewness, and kurtosis were, respectively, 0.73, 0.54, 4.25, and 37.4.

Several studies have been published in the literature to explore the effect of alkaline solutions on the engineering properties of FA-BGPC mixtures. For example, Hardjito et al. [130] carried out a laboratory experiment to demonstrate the influence of varied sodium silicate to sodium hydroxide ratios on the σ_c of FA-BGPC mixtures. They employed two different molarities and two different SS/SH ratios of 0.4 and 2.5. Their findings indicated that increasing the ratio of SS/SH significantly increased σ_c . For example, when the molarity was 8 M and the specimens were cured at 60 °C for approximately 24 h, the σ_c of FA-BGPC increased from 17.3 MPa to 56.8 MPa simply by increasing the ratio of SS/SH from 0.4 to 2.5. It was also discovered that changing the SS/SH ratio from 0.4 to 2.5 at a molarity of 14 M increased the σ_c from 47.9 MPa to 67.6 MPa [130].

Al-Azzawi et al. [60] showed an increase in the σ_c of FA-BGPC when the ratio of SS/SH rose in all geopolymer concrete mixtures, despite fly ash levels varying from 300 to 500 kg/m^3 . Similarly, Aliabdo et al. [68] evaluated the performance of FA-BGPC using three different SH/SS ratios of 0.3, 0.4, and 0.5. According to their findings, σ_c dropped as the SH/SS ratio grew, or compressive strength increased as the SS/SH ratio increased, as shown in Figure 16, the figure is adapted from [68]. The σ_c of the FA-BGPC has reduced by 22.5% and 29.5% at 0.4 and 0.5 SH/SS ratios, respectively, as compared to the SH/SS ratio of 0.3. Similar results have been reported in other investigations, despite different SS/SH being utilized [83,100,112,144].

Furthermore, Joseph and Mathew [87] carried out an experimental research study to investigate the effect of various parameters on the performance of FA-BGPC. It was observed that the σ_c increased with the increment of SS/SH ratio up to 2.5, and beyond that decline in the σ_c was reported, as shown in Figure 17, the figure is adapted from [87]. This result supported the theory that the microstructure of geopolymer concrete changes with the increment of the amount of sodium silicates, whereas the reduction in σ_c was attributed to the absence of a sufficient amount of sodium hydroxide in the mixture to complete the dissolution process during geopolymer formation [145,146], or due to the excess of OH^- concentration in the geopolymer concrete mixture [25]. On the other hand, some researchers thought that an overabundance of sodium could result in the formation

of sodium carbonate by air carbonation, interfering with the polymerization process and lowering compressive strength [131]. Another study was conducted in the same vein to study the impact of different SS/SH ratios on the σ_c of FA-BGPC. They utilized 0.5, 1.0, 1.5, 2.0, 2.5, and 3.0 as SS/SH ratios, and it was claimed that increasing the SS/SH ratio enhanced σ_c up to a ratio of SS/SH of 2.5 and thereafter lowered it [147]. However, several researchers found that the effect of the sodium silicate to sodium hydroxide ratio on the σ_c of geopolymer concrete was not noticeable [88,106].

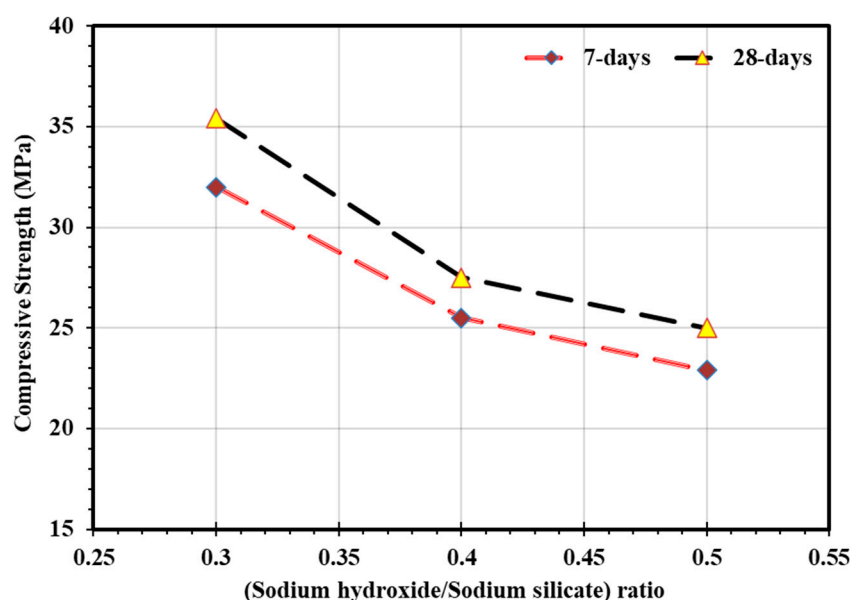


Figure 16. Effect of different SH/SS ratios on the σ_c of FA-BGPC at different curing ages.

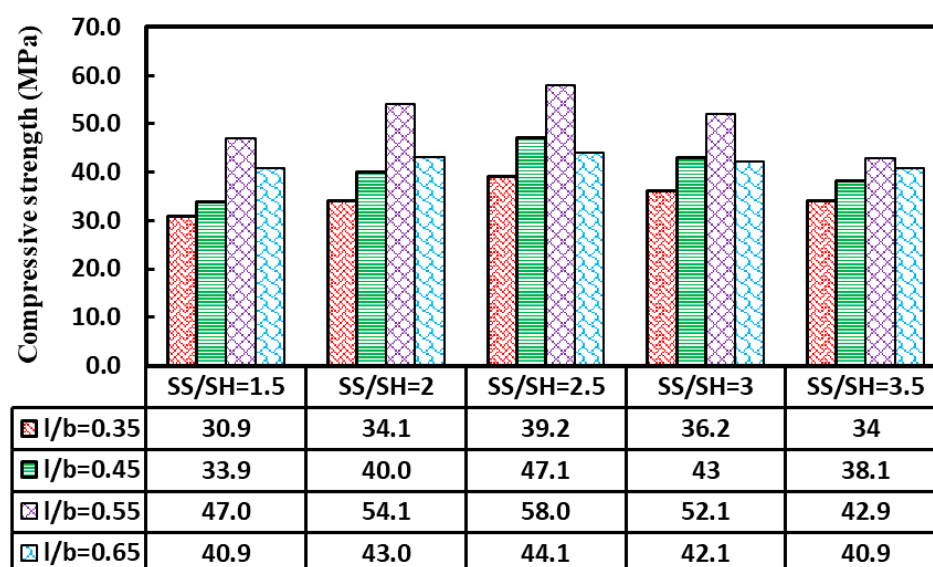


Figure 17. Effect of different SS/SH ratios on the σ_c of FA-BGPC. (Note: Total aggregate content = 70%, ratio of fine aggregate to total aggregate = 0.35, curing temperature = 100 °C, and period of heat curing inside oven = 24 h).

In contrast to the earlier results, fewer studies reported that the σ_c of FA-BGPC decreased as the ratio of sodium silicate to sodium hydroxide increased. For example, a study was carried out by Ghafoor et al. [105] to determine the influence of alkaline activators on the mechanical properties of FA-BGPC under ambient curing conditions. Their findings demonstrate that as the SS/SH ratio increased from 1.5 to 2, σ_c declined

by 5.2%, 7.6%, 7.6%, 10.8%, and 12.8%, respectively, for molarities of 8, 10, 12, 14, and 16. Similar patterns were observed when the SS/SH ratio was increased from 2 to 2.5, as shown in Figure 18, the figure is adapted from [105]. This result was explained by the fact that increasing the SS/SH ratio reduces the amount of sodium hydroxide solution and hydroxide ions (OH^-), which reduces the formation of N-A-S-H gels, which is the main 3D network that directly affects the microstructure of geopolymer concrete, and thus σ_c is reduced [148,149]. Similarly, Vora and Dave [102] documented a decrease in the σ_c of FA-BGPC as the SS/SH ratio was increased from 2 to 2.5. Furthermore, as the SS/SH ratio grew from 1.0 to 1.5, 2.0, and 2.5, the σ_c of fly ash-based geopolymer mortar decreased [150]. Therefore, it is suggested to use the ratio of SS/SH in the range of 1.5–2.5 for getting FA-BGPC with superior compressive strength.

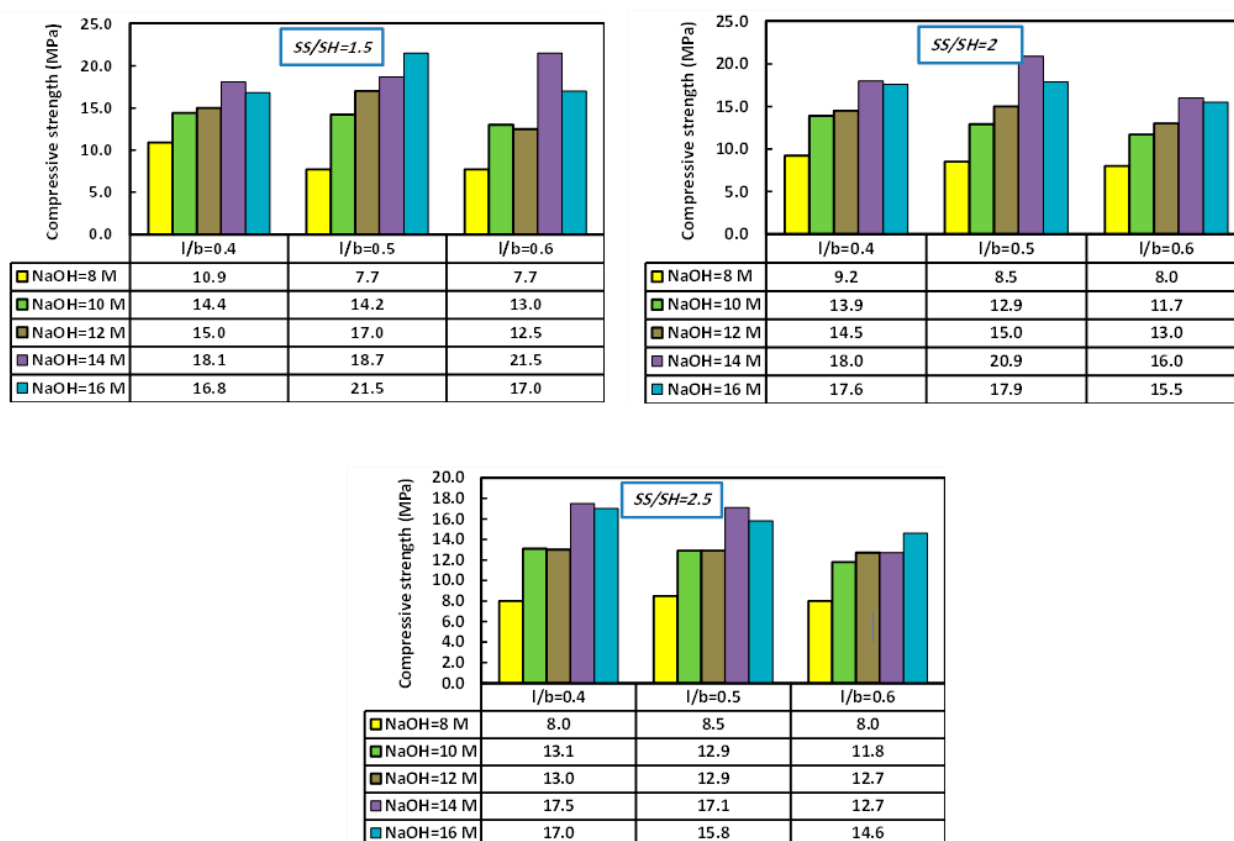


Figure 18. Effect of different SS/SH ratios on the σ_c of FA-BGPC at different M and l/b ratio.

4.7. Sodium Hydroxide Concentration (Molarity)

The concentration of sodium hydroxide is one of the critical parameters that affect the performance of FA-BGPC. Therefore, a wide range of studies has been done to highlight the effects of this issue. The sodium hydroxide concentration (molarity) ranged from 3 to 20 M, with an average of 12.05 M, a standard deviation of 2.88 M, a variance of 8.28, a skewness of 0.00, and kurtosis of -0.44 based on 800 dataset samples collected from prior studies.

An experimental laboratory research work was performed by Hardjito et al. [130] to demonstrate the influence of different molarities on the σ_c of FA-BGPC. At a ratio of SS/SH of 0.4, they found that σ_c improved by 176% for molarity of 14 M compared to molarity of 8 M, while, at a molarity of 14 M, this advantage was reduced to 19% when compared to molarity of 8 M at an SS/SH ratio of 2.5. In the same context, a research study has been carried out to evaluate the effect of different molarities on the σ_c of FA-BGPC. They observed that the σ_c was improved with the increment in the molarity of sodium hydroxide. For instance, σ_c improvement of 40% and 8% was reported when the concentration of sodium hydroxide changed from 8 M to 12 M and 12 M to

16 M, correspondingly [62]. This result was credited to an increase in sodium ions in the geopolymer concrete mixture, which was significant for the geopolymerization process because sodium ions were used to balance charges and build alumino-silicate networks from the source binder materials in the geopolymer concrete mixture [125,147]. On the other hand, at low molarity, the geopolymerization process is small due to the lower concentration of the base material. Consequently, a small amount of Si and Al are leached from the source binder materials [151].

Furthermore, Chithambaram et al. [64] did another experimental study to demonstrate the impacts of different molarities of sodium hydroxide on the mechanical properties of FA-BGPC. They used four different molarities at different curing temperatures and found that increasing the molarity promoted σ_c up to 12 M but decreased beyond that. For example, at the curing temperature of 90 °C and 28 days of age, the σ_c was 36, 38.5, 42.5, and 40.9 MPa for 8, 10, 12, and 14 molarities, respectively. Similarly, at 70 °C curing temperature, they reported σ_c of 33.8, 35.9, 40.5, and 39.4 MPa for 8, 10, 12, and 14 molarities, respectively. Additionally, they asserted that similar tendencies held true for curing temperatures of 60 and 80 °C. Similar results can also be observed in other studies even though different molarities were used [76,100]. However, Varaprasad et al. [152] claimed that the σ_c was improved with increased molarity. For example, they reported that the σ_c of FA-BGPC was improved by 8.5%, 14.7%, and 19.2% at 12, 14, and 16 molarities, respectively, compared to the molarity of 10 M at the age of 28 days with the curing temperature of 60°C. In the same manner, some other research studies claimed that the σ_c was improved as the molarity of sodium hydroxide increased [77,102,111,112].

According to the findings of Aliabdo et al. [68], the σ_c was increased as the molarity of sodium hydroxide increased in the FA-BGPC mixture up to 16 M, and then it decreased as depicted in Figure 19, the figure is adapted from [68]. In addition, they reported that the optimum concentration of NaOH was 16 M for 48 h of curing at 50°C. Moreover, Chindaprasirt and Chalee [153] discovered similar results when they employed various molarities of sodium hydroxide ranging from 8 to 20 M and recorded a maximum σ_c of 32.2 MPa at 16 M after 28 days of ambient curing. In the same context, a research study was carried out to demonstrate the influence of different NaOH molarities (10, 13, and 16 M) on the σ_c of FA-BGPC at elevated temperatures of 200, 400, 600, and 800°C. According to their findings, the σ_c was larger for specimens with higher molarities (13 and 16 M) at all temperature changes than specimens with 10 M NaOH solutions, as shown in Figure 20, the figure is adapted from [72]. On the other hand, they discovered that the rate of σ_c loss after 600 °C is also high in FA-BGPC mixtures with higher NaOH solution concentrations [72]. In addition, a study was carried out to see how different molarities of sodium hydroxide solutions (8, 10, 12, 14, and 16 M) affected the σ_c of FA-BGPC, and it was observed that the compressive strength of fly ash-based geopolymer concrete improved as the molarity of NaOH increased up to 10 M and then decreased, as shown in Figure 21, which is adapted from [87]. This is due to the fact that while the concentration of sodium hydroxide solution has a beneficial influence on hydrolysis, dissolution, and condensation processes during the manufacturing of geopolymer concrete while, overflowing alkali concentration prevents the condensation of silicate elements [145,146,154].

Finally, Ghafoor et al. [105] looked into the influence of alkaline activators on the mechanical properties of FA-BGPC when cured at room temperature. Their findings demonstrate that when the molarity of NaOH increased up to 14 M, the σ_c of FA-BGPC increased but then declined. For example, when the molarity of NaOH is changed from 8 to 10 M, 10 to 12 M, and 12 to 14 M, the σ_c improves by 55.8%, 10.5%, and 33%, respectively. However, when the concentration of sodium hydroxide increased from 14 M to 16 M, the compressive strength of the geopolymer concrete mixture decreased by around 9%.

In general, increasing the molarity of sodium hydroxide improves the σ_c of FA-BGPC composites, which could be attributed to the complete dissolution of aluminum and silicon particles during the polymerization process [144]. The larger the molarity of sodium

hydroxide, the more Al and Si particles dissolve, and as a result, the σ_c of geopolymer concrete mixtures increases [155].

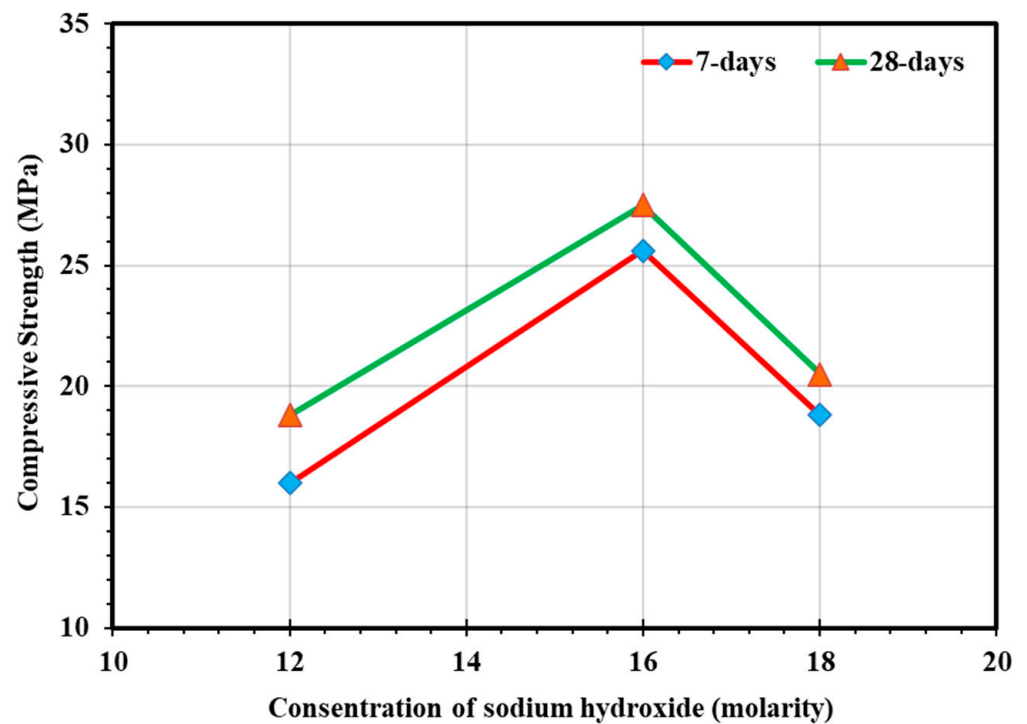


Figure 19. Impacts of different molarities of sodium hydroxide on the σ_c of FA-BGPC at the age of 7 and 28 days.

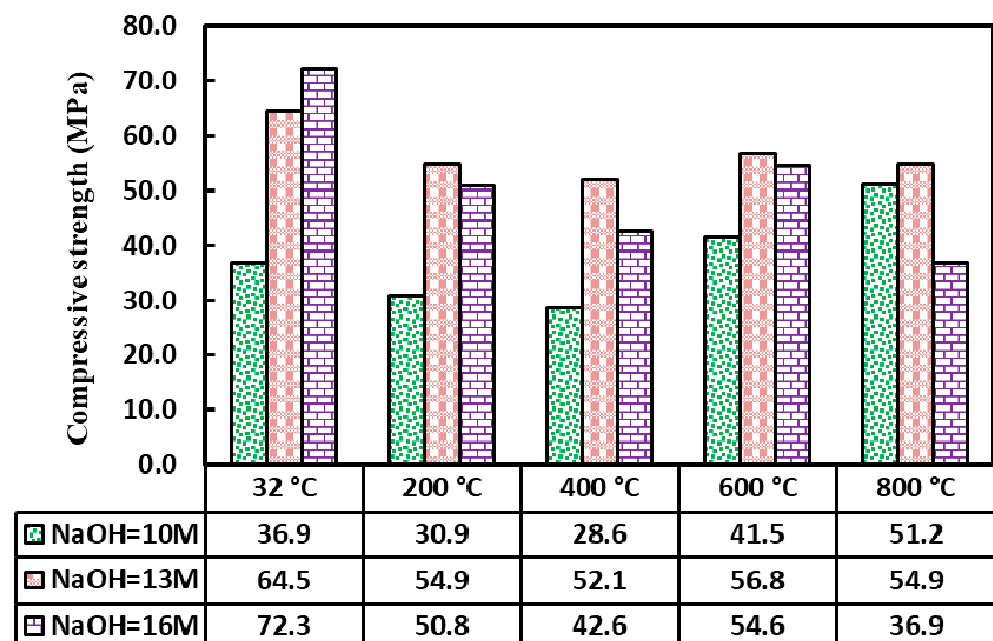


Figure 20. Impacts of different molarities of sodium hydroxide on the σ_c of FA-BGPC at various curing temperatures.

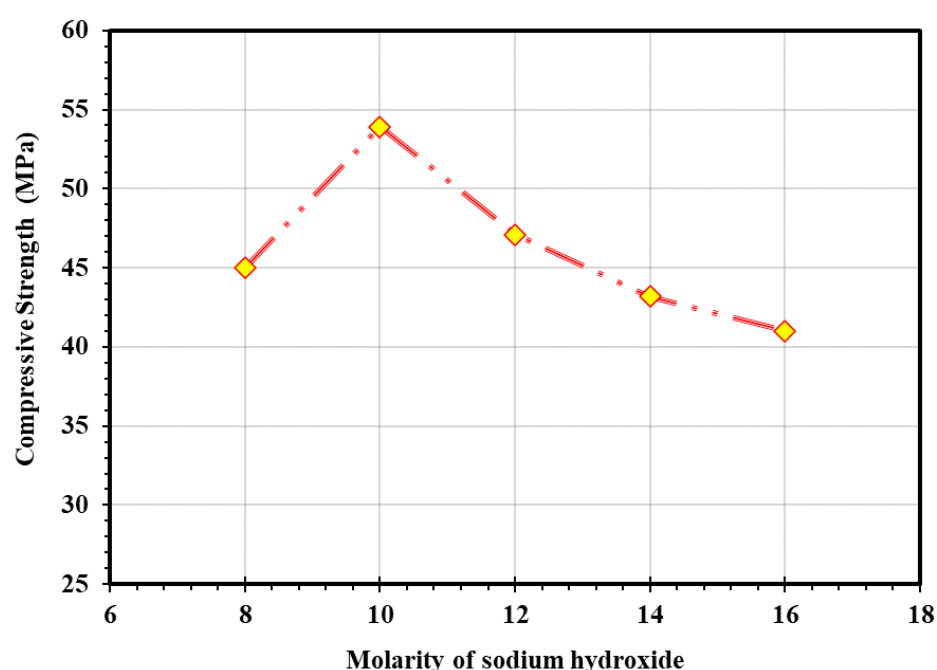


Figure 21. Impacts of different molarities of sodium hydroxide on the σ_c of FA-BGPC. (Note: Total aggregate content = 70%, ratio of fine aggregate to total aggregate = 0.35, SS/SH = 2.5, curing temperature = 100 °C, and period of heat curing inside oven = 24 h).

4.8. Curing Condition and Curing Ages

Generally, there are three different curing regimes for curing FA-BGPC composites: ambient curing, oven curing, and steam curing. The influence of these curing conditions on the σ_c of FA-BGPC was discussed in the following paragraph.

In comparison to other curing condition types, the majority of studies used oven curing conditions to cure the FA-BGPC and it was found that the most commonly utilized curing temperatures ranged from 60 to 80 °C.

Hardjito et al. [130] conducted research to determine the effect of various oven curing temperatures on the σ_c of FA-BGPC. Their results revealed that the σ_c was increased as the oven curing temperatures increased, as illustrated in Figure 22, the figure is adapted from [130]. However, this increase in the σ_c was not significant above the curing temperature of 60 °C. In addition, a study was carried out to demonstrate the impact of various curing conditions on the mechanical properties of FA-BGPC. At the ages of 3, 7, and 28 days, the σ_c of specimens cured under heat curing conditions was higher than that of specimens treated under ambient curing circumstances, as shown in Figure 23, the figure is adapted from [85]. For instance, at 90 °C oven curing temperature, the 28-day σ_c of FA-BGPC was 22.1 MPa, but at ambient curing temperature, it was 13.9 MPa [85]. Similar results can be found in other studies even though different ambient and oven curing temperatures were used [70,72,75,77,93,100,101,107,111,114].

In a similar vein, Chithambaram et al. [64] discovered that the σ_c of FA-BGPC increased as oven-cured temperatures climbed up to 90 °C and subsequently declined. For example, when the sodium hydroxide molarity in the concrete mixtures was 8 M, the σ_c at 28 days was 32.5, 33.8, 35.4, 36, and 33.9 MPa at 60, 70, 80, 90, and 100 °C oven curing temperatures, respectively. Similar trends were observed for ages 3 and 7 and for NaOH molarities of 10, 12, and 14 M. Similarly, Vora and Dave [102] found that increasing the oven curing temperature enhanced the σ_c of FA-BGPC mixtures. For example, when the oven curing temperature is increased from 60 to 75 °C and 75 to 90 °C, the σ_c increases by 21% and 6.5%, correspondingly.

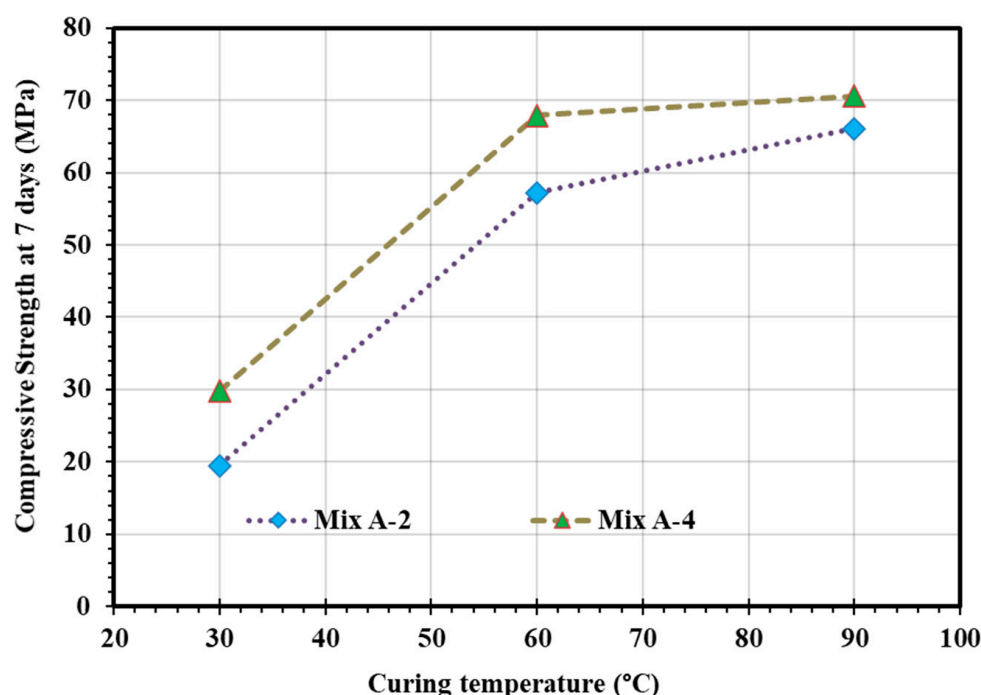


Figure 22. Effect of different oven curing temperatures on the σ_c of FA-BGPC. (Note: Mix A-2 has a molarity of 8 M, and SS/SH = 2.5, Mix A-4 has a molarity of 14 M, and SS/SH = 2.5).

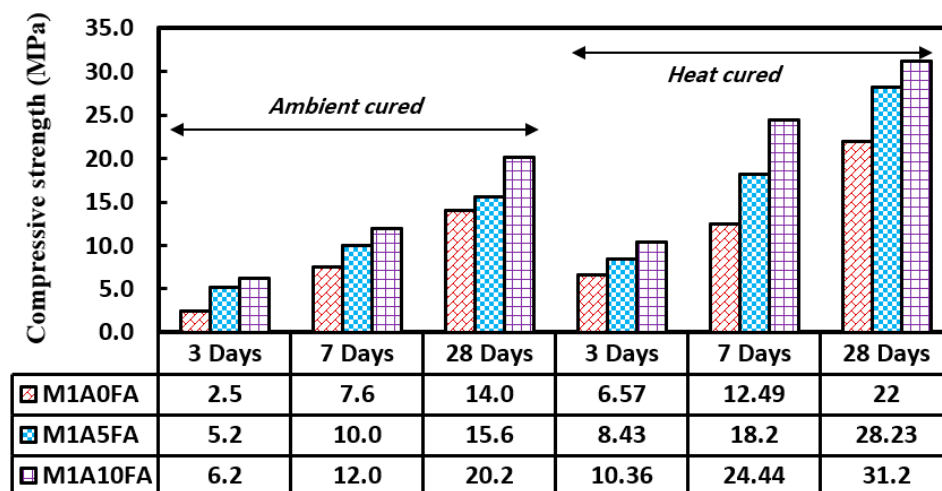


Figure 23. Effect of different curing conditions on the σ_c of FA-BGPC. (Note: M1 = fly ash content = 350 kg/m³, A = alccofine content, FA = fly ash).

Furthermore, an experimental laboratory study was carried out to see how the mechanical properties of FA-BGPC composites were affected by ambient and oven curing conditions. As demonstrated in Figure 24 (this figure is adapted from [93]), it was claimed that the σ_c enhancement for specimens cured under oven curing circumstances was larger than that for specimens cured under ambient curing regimes. This is because as the temperature of the geopolymer concrete specimens rises, the process of geopolymerization accelerates, and as a consequence, the σ_c improves [93].

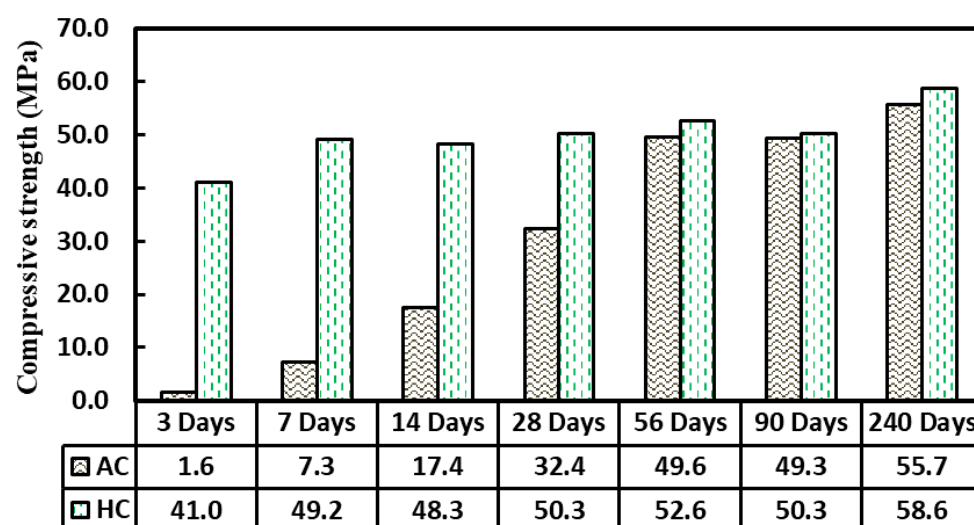


Figure 24. Influences of different curing conditions on the σ_c of FA-BGPC. (Note: AC = ambient cured, HC = heat cured).

Similarly, Joseph and Mathew [87] demonstrated that the σ_c of FA-BGPC increased with increasing oven curing temperatures up to 100 °C and declined thereafter, as illustrated in Figure 25, the figure is adapted from [87]. Additionally, they stated that this pattern held true for a variety of alkali solution to fly ash ratios. The drop in σ_c beyond 100 °C was attributed to moisture loss from the geopolymer concrete samples. Even when adequately sealed, at temperatures above 100 °C, the geopolymer samples may dry out, resulting in a fall in the σ_c . Similarly, Thakur and Ghosh [116] and Chindaprasirt et al. [153] found that increasing the oven curing temperature increased the σ_c of the geopolymer concrete composite.

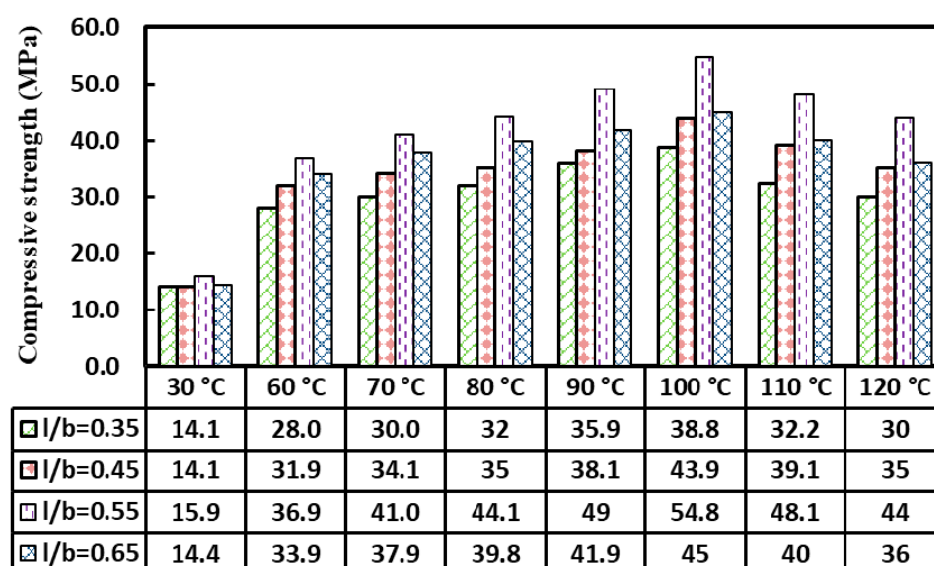


Figure 25. Influences of different oven curing temperatures on the σ_c of FA-BGPC. (Note: Total aggregate content = 70%, ratio of fine aggregate to total aggregate = 0.35, SS/SH = 2.5).

Furthermore, Hassan et al. [96] investigated the effect of curing conditions on the mechanical properties of FA-BGPC. They found that the σ_c of FA-BGPC at 7 and 28 days was in the range of 10.50–31.11 MPa for heat (75 °C) curing regimes, but it was reduced to 4.5–10 MPa for ambient curing regimes. In addition, they discovered that at 75 °C heat curing, the σ_c of FA-BGPC increased by 67% to ambient curing conditions after 28 days.

As illustrated in Figure 26 (adapted from [96]), a similar tendency was seen for varied ages of geopolymer concrete specimens. In the same vein, a study was done to determine the effect of ambient, steam, and heat curing conditions on the performance of FA-BGPC composites. Their findings suggested that the highest σ_c was obtained under heat curing conditions, followed by steam curing, and finally under ambient curing conditions. For instance, at the age of 3 days, the σ_c was 20.8, 16.7, and 8.75 MPa at heat, steam, and ambient curing conditions, correspondingly [109]. Another study, on the other hand, was done to demonstrate the effect of ambient, hot gunny sack, and external exposure curing regimes on the performance of FA-BGPC. They discovered that external exposure curing conditions resulted in a greater increase in σ_c than ambient curing conditions, whereas the worth curing condition was documented for hot gunny sack curing regimes [113].

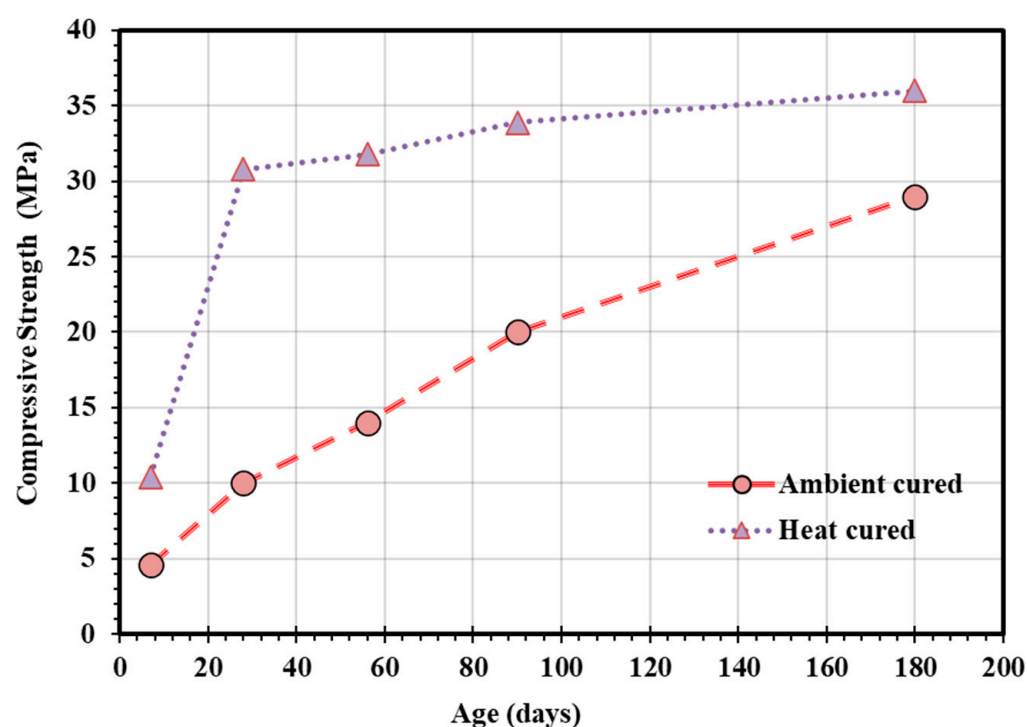


Figure 26. Impacts of different curing conditions on the σ_c of FA-BGPC at various curing ages.

Last but not least, one of the challenges that some researchers address is the period of curing FA-BGPC specimens within ovens. For example, a study was conducted by Thakur and Ghosh [116] to determine the effect of various mix compositions on the σ_c and microstructures of FA-BGPC composites. They revealed that the σ_c improved when the curing time inside the oven was increased at a steady temperature. After 48 h of thermal curing, the σ_c of FA-BGPC reached 40.8 MPa. They also discovered that increasing the curing time did not significantly increase the σ_c of FA-BGPC, as demonstrated in Figure 27, the figure is adapted from [116]. Similar results have been reported by Hardjito et al. [130]. On the other hand, Joseph and Mathew [87] declared that as the curing time inside the oven was increased at a constant temperature, the σ_c of FA-BGPC was enhanced. This increase in strength is proportional to the curing period, and a very small increase in strength can be acquired after 24 h, as illustrated in Figure 28, the figure is adapted from [87]. This result may be explained by the fact that most of the geopolymerization process occurs within 24 h.

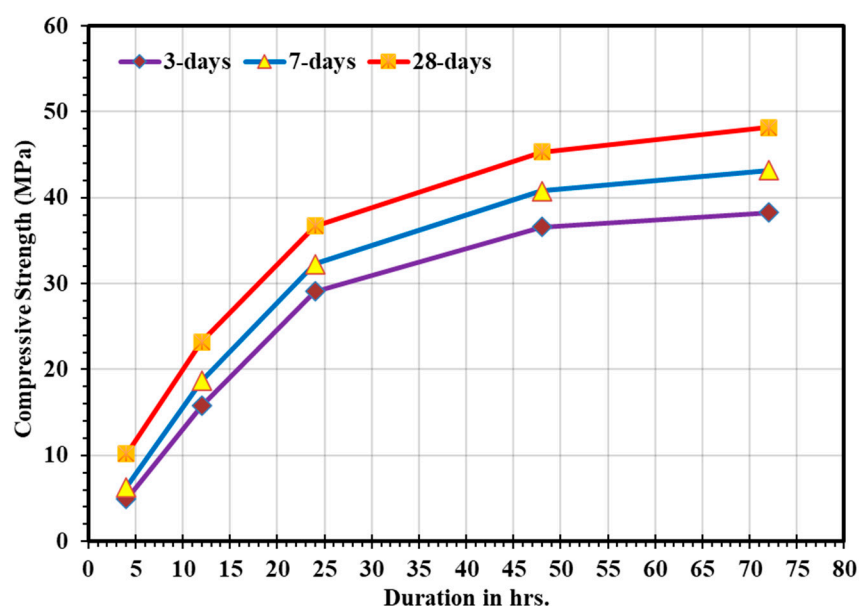


Figure 27. The effect of varying the temperature curing time inside an oven on the σ_c of FA-BGPC.

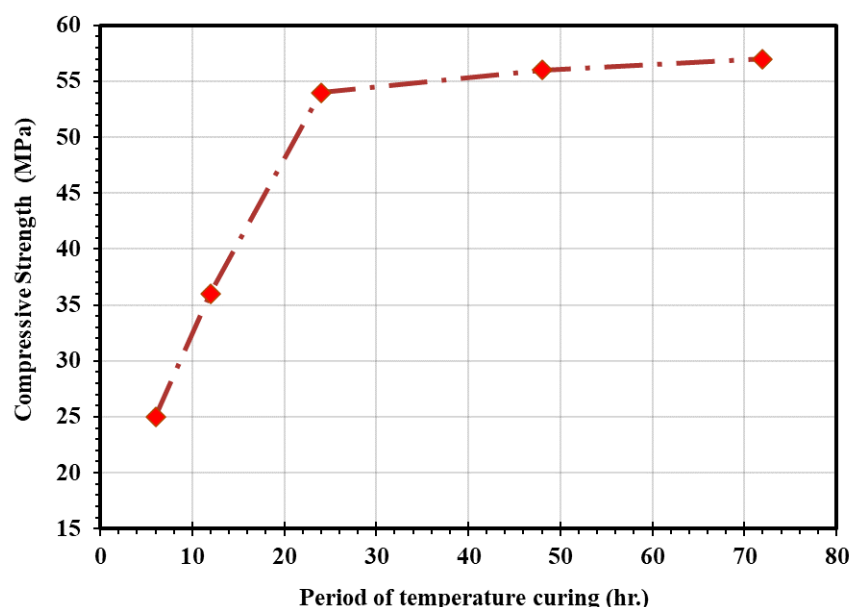


Figure 28. Impacts of varying the temperature curing time inside an oven on the σ_c of FA-BGPC. (Note: Total aggregate content = 70%, ratio of fine aggregate to total aggregate = 0.35, SS/SH = 2.5, curing temperature = 100 °C).

5. Research Needs

Studies on the various properties of fly ash-based geopolymer concrete composites are a thriving field with both outstanding intellectual merits and significant broader implications. More fundamental research on the potential of this type of sustainable concrete composite is currently needed to broaden scholars' horizons and to be used by the construction industry. The objective is to develop a mechanistic understanding of FA-BGPCs' rheological, hydration, or polymerization process and in-service behaviors. Detailed laboratory and field investigations are needed to gather a massive amount of data on the engineering properties of FA-BGPC composites and their durability in various service environments and lay the groundwork for their specification and use by practicing engineers.

A variety of codes and standards governs traditional concrete. These relationships between strengths are based on a wealth of data on various engineering properties and

developed over decades. Geopolymer concrete has been studied less extensively than traditional concrete, and quantitative data on its durability and mechanical properties are lacking. However, Mohammed et al. [19] developed empirical equations for geopolymer concrete composites, but their equations were designed for a wide range of data with different source binder materials, curing conditions, and various mixture proportion parameters; therefore, it is suggested to develop equations for predicting the most important mechanical properties of geopolymer concrete such as splitting tensile strength, flexural strength, and modulus elasticity based on their compressive strength results. This issue needs a considerable amount of data in the same condition because, unlike conventional concrete, geopolymer concrete is affected by a wide range of parameters as discussed in detail in this study.

Geopolymer concrete is a technique that is rarely used in large-scale engineering projects, while it is mostly accepted and familiar in academic and research circles. There are barriers to industrial application, such as geopolymers using various raw materials, and developing and certifying the raw materials requires significant investment. The construction and manufacturing industries are conservative in their approach to product adoption. In developed countries, particular performance standards for the binder are in place. As a result, products such as geopolymer concrete may not be entirely acceptable, as geopolymer concrete does not fully comply with regulatory standards, most notably in terms of rheology and chemical composition. This can be a significant impediment to geopolymer concrete adoption. Further, there is a shortage of research on the mechanical properties of FA-BGPC at room temperature. Thus, additional studies at ambient temperature are required to ensure that the FA-BGPC can be used extensively in cast-in-situ concrete applications.

A few researchers have proposed some changes to the existing traditional concrete mix design for geopolymer concrete. However, it is necessary to establish an optimal mix proportioning and design for geopolymer concrete for getting the required compressive strength of FA-BGPC like ACI 211 [156]; thus, standardization of testing methods, technical indicators, and performance-based specifications directly applicable to geopolymer products are essential works that needs further efforts, and further research into the new application area and the establishment of an evaluation system for geopolymer-related products are required. On the other hand, there are studies available on the effect of curing temperature, curing duration, rest period, the molarity of NaOH, and the ratio of $\text{Na}_2\text{SiO}_3/\text{NaOH}$ on the properties of geopolymer concrete. However, the optimal values for these parameters must be determined in order to achieve the desired level of FA-BGPC strength.

Geopolymerization involves a complex chemical process and our understanding of it is still developing. Therefore, it is recommended to conduct more and more studies to clarify the geopolymerisation process as well as the polymerization products, which are the main issues that govern the compressive strength of geopolymer concrete composites.

Last but not least, it is essential for studies to be carried out to investigate materials properties of geopolymer composites such as nonlinear viscoelastic-viscoplastic with hardening-relaxation constitutive relationship for geopolymer mixtures as these issues were successfully studied for asphalt mixtures [157,158]. In addition, trying to improve materials properties by adding newly developed additives such as styrene-butadiene-styrene (SBS) or Evotherm-M1 is one of the other essential works that researchers in this field should adequately investigate, because these additives were significantly improved engineering properties of asphaltic mixtures [159]. Furthermore, geopolymer concrete behavior in multi-axial stress states, stiffness degradation, and recovery should be studied further to better understand the structural behavior of geopolymer concrete. Finally, geopolymer concrete is a brittle material with low tensile strength, just like conventional concrete. This issue was adequately and extensively studied for traditional concrete by using steel bars and various types of fibers [160], while more research is essential in the case of FA-BGPC.

6. Discussion

- I. As a result of the above systematic comprehensive review of the literature, geopolymer concrete can be defined as cementless concrete that uses industrial or agro by-product ashes as the main binder instead of ordinary Portland cement, making it an eco-efficient and environmentally friendly construction material. This type of concrete is affected by many mixed proportion parameters as well as curing conditions. Further, this type of concrete reduces energy consumption, waste disposal, and construction cost.
- II. The alkaline solution to binder ratio (l/b) is the sum of sodium hydroxide and sodium silicate content to the entire weight or volume of the fly ash or other source binder materials in the mixture proportions of the geopolymer concrete mixtures. This ratio has a considerable impact on the σ_c of the FA-BGPC. According to several studies, the σ_c improved as the l/b increased up to a certain point, then dropped. However, on the other hand, some researchers noticed a decrease in σ_c as the l/b was raised. Decreasing l/b ratio will lead to accelerating in the alkaline activation process of FA-BGPC due to the decrease of consistency of the geopolymer concrete mixture, and in this case, the calcium aluminate silicate hydrate (C-A-S-H) gel and sodium aluminate silicate hydrate (N-A-S-H) gel can be generated quickly in the geopolymer concrete mixture, and as a consequence participated in the development of early-age σ_c of FA-BGPC. Therefore, it is suggested to use the ratio of l/b in the range of 0.35 to 0.55 for getting an FA-BGPC mixture with the required workability and strength.
- III. Superplasticizer and water content are two key parameters that govern the workability behavior of the FA-BGPC and hence affect the hardened characteristics of the geopolymer concrete. Like conventional concrete, increasing water content or extra water to the FA-BGPC will lead to decreasing the σ_c of the geopolymer concrete. This is due to water evaporation in the geopolymer concrete mixture, which results in the formation of pores and cavities within the geopolymer concrete matrix as the geopolymer concrete specimens cure at high temperatures within ovens. Furthermore, excess water may affect the alkalinity environment of the fly ash-based geopolymer concrete matrix, thereby slowing the polymerization process between the alkaline and source materials. While the addition of a superplasticizer increases the σ_c of FA-BGPC composites up to a point, and it has a detrimental influence on σ_c above that point.
- IV. Fly ash is one of the most common types of source material binders to produce geopolymer concrete composites. The amount of fly ash content in the geopolymer concrete mixture influences the composite's σ_c . As the fly ash content increased in the geopolymer concrete mixture, the σ_c was improved. This is because the higher content of fly ash in the geopolymer concrete mixture gives a denser and compacted microstructure to the geopolymer concrete matrix. Moreover, the particles of fly ash facilitate movement among the aggregate particles owing to the spherical shape and smooth surface of the particles of fly ash; on the other hand, the volume of fine fraction particles in the geopolymer concrete matrix increased as the fly ash content increased, thus, in turn, fill the voids and pores between the aggregate particles and hence σ_c was improved. In addition, fly ash is the main source of aluminosilicate source materials in the geopolymer concrete mixture, which silica and alumina increase as the amount of fly ash content increases; thus, they affect the reactions in the polymerization process, which, in turn, increased C-A-S-H and N-A-S-H gels, and finally, σ_c was improved.
- V. Fine and coarse aggregates have the same effect on the performance of geopolymer concrete mixtures as they do on conventional concrete mixtures. As a result, it was proposed that good aggregate quality be used to make good geopolymer concrete composites and that roughly 65–75% aggregate content be used to make 1.0 m³ of FA-BGPC.

- VI. The amount of alkaline solution and the ratio of sodium silicate to sodium hydroxide (SS/SH) considerably affect the σ_c of FA-BGPC. The σ_c of FA-BGPC increases as the ratio of SS/SH increases up to a limited amount; this increase in the σ_c is due to the improvement in the microstructure of geopolymer concrete at the required quantity of sodium silicates content, while, at a high ratio of SS/SH, reduction in the σ_c happened due to the fact that there is not a sufficient amount of sodium hydroxide present in the mixture to completion of dissolution process during the formation of geopolymer or due to the excess OH^- concentration in the geopolymer concrete mixture. On the other hand, the excess of the sodium content can form sodium carbonate by atmospheric carbonation, and this may disrupt the polymerization process, and as a result, σ_c was decreased. Therefore, it is suggested to use the ratio of SS/SH in the range of 1.5–2.5 for getting FA-BGPC with superior σ_c .
- VII. The value of the concentration of sodium hydroxide solution has an appreciable effect on the σ_c of FA-BGPC. Because it leads to increased sodium ions in the geopolymer concrete mixture, which was significant for the polymerization process, sodium ions were used to balance the charges and formed alumino-silicate networks as a source materials binder in the geopolymer concrete mixture. Therefore, it was suggested to use the molarity of sodium hydroxide in the range of 10–16 M to produce the FA-BGPC mixtures with acceptable σ_c behavior.
- VIII. The σ_c of FA-BGPC is significantly affected by the curing temperature and duration. Longer curing time and curing at high temperatures (50–100 °C) increases the σ_c of FA-BGPC, although the increase in strength may be insignificant for curing at more than 60 °C and for periods longer than 48 h. Therefore, for heat curing regimes, temperatures between 50–80 °C and curing time of 24 h are widely accepted values for a successful polymerization process. In addition, among the curing condition methods (oven, steam, and ambient), oven curing techniques better influence the σ_c of FA-BGPC composites.

7. Conclusions

Based on the extensive literature review and discussions made in this study, the following conclusions can be reached:

- I. Geopolymer concrete with acceptable σ_c values could be produced by using fly ash as source binder materials.
- II. The alkaline solution to the binder ratio (l/b) significantly impacts the σ_c of the FA-BGPC. Some researchers believe that the σ_c was improved as the l/b increased. At the same time, the reduction in the σ_c was reported by many researchers as the l/b was increased.
- III. Increasing water content or extra water in the FA-BGPC will decrease the σ_c of the geopolymer concrete. In comparison, superplasticizer content improves σ_c of the FA-BGPC composites up to a limited value of around 2.5% of fly ash content.
- IV. The σ_c of FA-BGPC increases as the ratio of SS/SH increases up to around 2.5, then decreases.
- V. It was suggested to use the molarity of sodium hydroxide in the range of 10–16 M to produce the FA-BGPC mixtures with acceptable σ_c behavior.
- VI. Among the curing methods, the heat curing regime is the best one for getting early and high σ_c in FA-BGPC.
- VII. It was suggested to use the oven curing temperatures between 50–80 °C and curing time of 24 h for a successful polymerization process and getting acceptable σ_c in FA-BGPC.

Recommendation: Detailed investigations on fly ash-based geopolymer concrete's fresh and mechanical properties can be found in the literature. However, studies which are focused on the other properties of this composite are still limited. For this composite to be acceptable by the construction industry, some durability properties such as water

permeability, gas permeability, chloride resistance, and freeze-thaw resistance should be examined comprehensively. Finally, the fatigue performance of fly ash-based geopolymer concrete needs more research and experimental investigations.

Author Contributions: Conceptualization, H.U.A.; methodology, H.U.A., A.A.M., S.R., A.S.M., A.M., S.M.A.Q. and N.H.S.; software H.U.A., A.A.M., S.R., A.S.M., A.M., S.M.A.Q. and N.H.S.; validation, A.A.M., S.R., A.S.M., A.M., S.M.A.Q. and N.H.S.; formal analysis, H.U.A., A.A.M. and A.S.M.; investigation, H.U.A.; resources, A.M.; data curation, H.U.A., A.A.M., S.R., A.S.M., A.M., S.M.A.Q. and N.H.S.; writing—original draft preparation, H.U.A., A.A.M., S.R., A.S.M., A.M., S.M.A.Q. and N.H.S.; writing—review and editing, H.U.A., A.A.M., S.R., A.S.M., A.M., S.M.A.Q. and N.H.S.; visualization, H.U.A., A.A.M., S.R., A.S.M., A.M., S.M.A.Q. and N.H.S.; supervision, A.A.M., S.R., A.S.M. and A.M.; project administration, H.U.A., A.A.M., A.S.M. and A.M.; funding acquisition, A.M. All authors have read and agreed to the published version of the manuscript.

Funding: This research received no external funding.

Institutional Review Board Statement: Not applicable.

Informed Consent Statement: Not applicable.

Data Availability Statement: The data presented in this study are available on request from the corresponding author.

Conflicts of Interest: The authors declare no conflict of interest.

References

1. Mahasenan, N.; Smith, S.; Humphreys, K. The cement industry and global climate change: Current and potential future cement industry CO₂ emissions. In *Greenhouse Gas Control Technologies-6th International Conference*; Elsevier: Pergamon, Turkey, 2003; pp. 995–1000.
2. Madheswaran, C.K.; Gnanasundar, G.; Gopalakrishnan, N. Effect of molarity in geopolymer concrete. *Int. J. Civ. Struct. Eng.* **2013**, *4*, 106–115.
3. Yu, Q.L. Application of nanomaterials in alkali-activated materials. In *Nanotechnology in Eco-Efficient Construction*; Woodhead Publishing: Sawston, UK, 2019; pp. 97–121.
4. Guo, X.; Shi, H.; Dick, W.A. Compressive strength and microstructural characteristics of class C fly ash geopolymer. *Cem. Concr. Compos.* **2010**, *32*, 142–147. [[CrossRef](#)]
5. Mehta, P.K. Reducing the environmental impact of concrete. *Concr. Int.* **2001**, *23*, 61–66.
6. Mejeoumov, G.G. *Improved Cement Quality and Grinding Efficiency by Means of Closed Mill Circuit Modeling*; Texas A&M University: College Station, TX, USA, 2007.
7. Shaikh, F.U.A. Mechanical and durability properties of fly ash geopolymer concrete containing recycled coarse aggregates. *Int. J. Sustain. Built Environ.* **2016**, *5*, 277–287. [[CrossRef](#)]
8. Shalini, A.; Gurunaryanan, G.; Sakthivel, S. Performance of rice husk ash in geopolymer concrete. *Int. J. Innov. Res. Sci. Tech.* **2016**, *2*, 73–77.
9. Han, B.; Yu, X.; Ou, J. *Self-Sensing Concrete in Smart Structures*; Butterworth-Heinemann: Oxford, UK, 2014.
10. Provis, J.L.; Palomo, A.; Shi, C. Advances in understanding alkali-activated materials. *Cem. Concr. Res.* **2015**, *78*, 110–125. [[CrossRef](#)]
11. Abdel-Gawwad, H.A.; Abo-El-Enein, S.A. A novel method to produce dry geopolymer cement powder. *HBRC J.* **2016**, *12*, 13–24. [[CrossRef](#)]
12. Davidovits, J. *Geopolymer Chemistry and Applications*, 4th ed.; Geopolymer Institute: Saint-Quentin, France, 2015.
13. Davidovits, J. *Geopolymer Chemistry and Application*, 2nd ed.; Geopolymer Institute: Saint-Quentin, France, 2008.
14. Palomo, A.; Grutzeck, M.W.; Blanco, M.T. Alkali-activated fly ashes: A cement for the future. *Cem. Concr. Res.* **1999**, *29*, 1323–1329. [[CrossRef](#)]
15. Abdullah, M.M.A.; Hussin, K.; Bnhussain, M.; Ismail, K.N.; Ibrahim, W.M.W. Mechanism and chemical reaction of fly ash geopolymer cement—A review. *Int. J. Pure Appl. Sci. Technol.* **2011**, *6*, 35–44.
16. Liew, Y.M.; Heah, C.Y.; Kamarudin, H. Structure and properties of clay-based geopolymer cements: A review. *Prog. Mater. Sci.* **2016**, *83*, 595–629. [[CrossRef](#)]
17. Duxson, P.; Fernández-Jiménez, A.; Provis, J.L.; Lukey, G.C.; Palomo, A.; van Deventer, J.S. Geopolymer technology: The current state of the art. *J. Mater. Sci.* **2007**, *42*, 2917–2933. [[CrossRef](#)]
18. Ravitheja, A.; Kumar, N.K. A study on the effect of nano clay and GGBS on the strength properties of fly ash based geopolymers. *Mater. Today Proc.* **2019**, *19*, 273–276. [[CrossRef](#)]
19. Mohammed, A.A.; Ahmed, H.U.; Mosavi, A. Survey of Mechanical Properties of Geopolymer Concrete: A Comprehensive Review and Data Analysis. *Materials* **2021**, *14*, 4690. [[CrossRef](#)] [[PubMed](#)]

20. Diaz, E.I.; Allouche, E.N.; Eklund, S. Factors affecting the suitability of fly ash as source material for geopolymers. *Fuel* **2010**, *89*, 992–996. [\[CrossRef\]](#)
21. Yip, C.K.; Lukey, G.C.; Provis, J.L.; van Deventer, J.S. Effect of calcium silicate sources on geopolymerisation. *Cem. Concr. Res.* **2008**, *38*, 554–564. [\[CrossRef\]](#)
22. Sumesh, M.; Alengaram, U.J.; Jumaat, M.Z.; Mo, K.H.; Alnahhal, M.F. Incorporation of nano-materials in cement composite and geopolymer based paste and mortar—A review. *Constr. Build. Mater.* **2017**, *148*, 62–84. [\[CrossRef\]](#)
23. Weil, M.; Dombrowski, K.; Buchwald, A. Life-cycle analysis of geopolymer. In *Geopolymers*; Woodhead Publishing: Sawston, UK, 2009; pp. 194–210.
24. Omer, S.A.; Demirboga, R.; Khushefati, W.H. Relationship between compressive strength and UPV of GGBFS based geopolymer mortars exposed to elevated temperatures. *Constr. Build. Mater.* **2015**, *94*, 189–195. [\[CrossRef\]](#)
25. Feng, Y.; Zhang, Q.; Chen, Q.; Wang, D.; Guo, H.; Liu, L.; Yang, Q. Hydration and strength development in blended cement with ultrafine granulated copper slag. *PLoS ONE* **2019**, *14*, e0215677. [\[CrossRef\]](#) [\[PubMed\]](#)
26. Pavithra, P.E.; Reddy, M.S.; Dinakar, P.; Rao, B.H.; Satpathy, B.K.; Mohanty, A.N. A mix design procedure for geopolymer concrete with fly ash. *J. Clean. Prod.* **2016**, *133*, 117–125. [\[CrossRef\]](#)
27. Gorai, B.; Jana, R.K. Characteristics and utilisation of copper slag—A review. *Resour. Conserv. Recycl.* **2003**, *39*, 299–313. [\[CrossRef\]](#)
28. Ahmaruzzaman, M. A review on the utilization of fly ash. *Prog. Energy Combust. Sci.* **2010**, *36*, 327–363. [\[CrossRef\]](#)
29. ASTM-C618. *Standard Specification for Coal Fly Ash and Raw or Calcined Natural Pozzolan for Use as a Mineral Admixture in Concrete*; ASTM International: West Conshohocken, PA, USA, 1999.
30. Bankowski, P.; Zou, L.; Hodges, R. Reduction of metal leaching in brown coal fly ash using geopolymers. *J. Hazard. Mater.* **2004**, *114*, 59–67. [\[CrossRef\]](#) [\[PubMed\]](#)
31. Antiohos, S.K.; Tsimas, S. A novel way to upgrade the coarse part of a high calcium fly ash for reuse into cement systems. *Waste Manag.* **2007**, *27*, 675–683. [\[CrossRef\]](#) [\[PubMed\]](#)
32. Neupane, G.; Donahoe, R.J. Leachability of elements in alkaline and acidic coal fly ash samples during batch and column leaching tests. *Fuel* **2013**, *104*, 758–770. [\[CrossRef\]](#)
33. Nyale, S.M.; Eze, C.P.; Akinyeye, R.O.; Gitari, W.M.; Akinyemi, S.A.; Fatoba, O.O.; Petrik, L.F. The leaching behaviour and geochemical fractionation of trace elements in hydraulically disposed weathered coal fly ash. *J. Environ. Sci. Health* **2014**, *49*, 233–242. [\[CrossRef\]](#) [\[PubMed\]](#)
34. Yao, Z.T.; Ji, X.S.; Sarker, P.K.; Tang, J.H.; Ge, L.Q.; Xia, M.S.; Xi, Y.Q. A comprehensive review on the applications of coal fly ash. *Earth-Sci. Rev.* **2015**, *141*, 105–121. [\[CrossRef\]](#)
35. Shibayama, A.; Kim, Y.; Harjanto, S.; Sugai, Y.; Okada, K.; Fujita, T. Remediation of contaminated soil by fly ash containing dioxins from incineration by using flotation. *Mater. Trans.* **2005**, *46*, 990–995. [\[CrossRef\]](#)
36. Nomura, Y.; Fujiwara, K.; Terada, A.; Nakai, S.; Hosomi, M. Prevention of lead leaching from fly ashes by mechanochemical treatment. *Waste Manag.* **2010**, *30*, 1290–1295. [\[CrossRef\]](#) [\[PubMed\]](#)
37. Boiny, H.U.; Alshkane, Y.M.; Rafiq, S.K. Mechanical properties of cement mortar by using polyethylene terephthalate fibers. In Proceedings of the 5th National and 1st International Conference on Modern Materials and Structures in Civil Engineering, Tehran, Iran, 26–27 October 2016.
38. Alshkane, Y.M.; Rafiq, S.K.; Boiny, H.U. Correlation between Destructive and Non-Destructive Tests on the Mechanical Properties of Different Cement Mortar Mixtures incorporating Polyethylene Terephthalate Fibers. *Sulaimania J. Eng. Sci.* **2017**, *4*, 67–73. [\[CrossRef\]](#)
39. Ahmed, H.U.; Faraj, R.H.; Hilal, N.; Mohammed, A.A.; Sherwani, A.F.H. Use of recycled fibers in concrete composites: A systematic comprehensive review. *Compos. Part B Eng.* **2021**, *215*, 108769. [\[CrossRef\]](#)
40. Bouzoubaa, N.; Lachemi, M. Self-compacting concrete incorporating high volumes of class F fly ash: Preliminary results. *Cem. Concr. Res.* **2001**, *31*, 413–420. [\[CrossRef\]](#)
41. Dinakar, P.; Babu, K.G.; Santhanam, M. Mechanical properties of high-volume fly ash self-compacting concrete mixtures. *Struct. Concr.* **2008**, *9*, 109–116. [\[CrossRef\]](#)
42. Barbhuiya, S. Effects of fly ash and dolomite powder on the properties of self-compacting concrete. *Constr. Build. Mater.* **2011**, *25*, 3301–3305. [\[CrossRef\]](#)
43. Ahmed, H.U. Influence of Hydrated Lime Addition on Self-Healing Capability of High-Volume Fly Ash Incorporated Cementitious Composites. Master's Thesis, Hasan Kalyoncu University, Gaziantep, Turkey, 2014.
44. Yildirim, G.; Sahmaran, M.; Ahmed, H.U. Influence of hydrated lime addition on the self-healing capability of high-volume fly ash incorporated cementitious composites. *J. Mater. Civ. Eng.* **2015**, *27*, 04014187. [\[CrossRef\]](#)
45. Moffatt, E.G.; Thomas, M.D.; Fahim, A. Performance of high-volume fly ash concrete in marine environment. *Cem. Concr. Res.* **2017**, *102*, 127–135. [\[CrossRef\]](#)
46. Anjos, M.A.; Camões, A.; Campos, P.; Azeredo, G.A.; Ferreira, R.L. Effect of high volume fly ash and metakaolin with and without hydrated lime on the properties of self-compacting concrete. *J. Build. Eng.* **2020**, *27*, 100985. [\[CrossRef\]](#)
47. Roychand, R.; Li, J.; De Silva, S.; Saberian, M.; Law, D.; Pramanik, B.K. Development of zero cement composite for the protection of concrete sewage pipes from corrosion and fatbergs. *Resour. Conserv. Recycl.* **2021**, *164*, 105166. [\[CrossRef\]](#)

48. Jiang, X.; Xiao, R.; Ma, Y.; Zhang, M.; Bai, Y.; Huang, B. Influence of waste glass powder on the physico-mechanical properties and microstructures of fly ash-based geopolymer paste after exposure to high temperatures. *Constr. Build. Mater.* **2020**, *262*, 120579. [\[CrossRef\]](#)
49. Wulandari, K.D.; Ekaputri, J.J.; Kurniawan, S.B.; Primaningtyas, W.E.; Abdullah, S.R.S.; Ismail, N.I.; Imron, M.F. Effect of microbes addition on the properties and surface morphology of fly ash-based geopolymer paste. *J. Build. Eng.* **2021**, *33*, 101596. [\[CrossRef\]](#)
50. Shill, S.K.; Al-Deen, S.; Ashraf, M.; Hutchison, W. Resistance of fly ash based geopolymer mortar to both chemicals and high thermal cycles simultaneously. *Constr. Build. Mater.* **2020**, *239*, 117886. [\[CrossRef\]](#)
51. Sivasakthi, M.; Jeyalakshmi, R.; Rajamane, N.P. Fly ash geopolymer mortar: Impact of the substitution of river sand by copper slag as a fine aggregate on its thermal resistance properties. *J. Clean. Prod.* **2021**, *279*, 123766. [\[CrossRef\]](#)
52. Noushini, A.; Castel, A.; Aldred, J.; Rawal, A. Chloride diffusion resistance and chloride binding capacity of fly ash-based geopolymer concrete. *Cem. Concr. Compos.* **2020**, *105*, 103290. [\[CrossRef\]](#)
53. Morla, P.; Gupta, R.; Azarsa, P.; Sharma, A. Corrosion Evaluation of Geopolymer Concrete Made with Fly Ash and Bottom Ash. *Sustainability* **2021**, *13*, 398. [\[CrossRef\]](#)
54. Ahmed, H.U.; Mohammed, A.S.; Mohammed, A.A.; Faraj, R.H. Systematic multiscale models to predict the compressive strength of fly ash-based geopolymer concrete at various mixture proportions and curing regimes. *PLoS ONE* **2021**, *16*, e0253006. [\[CrossRef\]](#) [\[PubMed\]](#)
55. Zhuang, X.Y.; Chen, L.; Komarneni, S.; Zhou, C.H.; Tong, D.S.; Yang, H.M.; Yu, W.H.; Wang, H. Fly ash-based geopolymer: Clean production, properties and applications. *J. Clean. Prod.* **2016**, *125*, 253–267. [\[CrossRef\]](#)
56. Ouyang, X.; Ma, Y.; Liu, Z.; Liang, J.; Ye, G. Effect of the sodium silicate modulus and slag content on fresh and hardened properties of alkali-activated fly ash/slag. *Minerals* **2020**, *10*, 15. [\[CrossRef\]](#)
57. Neville, A.M.; Brooks, J.J. *Concrete Technology*; Longman Scientific & Technical: London, UK, 2010.
58. ASTM C39/C39M. *Standard Test Method for Compressive Strength of Cylindrical Concrete Specimens*; ASTM International: West Conshohocken, PA, USA, 2017.
59. Hardjito, D.; Wallah, S.E.; Sumajouw, D.M.J.; Rangan, B.V. Introducing fly ash-based geopolymer concrete: Manufacture and engineering properties. In Proceedings of the 30th Conference on Our World in Concrete & Structures, Singapore, 23–24 August 2005; Volume 24.
60. Al-Azzawi, M.; Yu, T.; Hadi, M.N. Factors affecting the bond strength between the fly ash-based geopolymer concrete and steel reinforcement. In *Structures*; Elsevier: Amsterdam, The Netherlands, 2018; Volume 14, pp. 262–272.
61. Zhao, R.; Yuan, Y.; Cheng, Z.; Wen, T.; Li, J.; Li, F.; Ma, Z.J. Freeze-thaw resistance of class F fly ash-based geopolymer concrete. *Constr. Build. Mater.* **2019**, *222*, 474–483. [\[CrossRef\]](#)
62. Singhal, D.; Junaid, M.T.; Jindal, B.B.; Mehta, A. Mechanical and microstructural properties of fly ash based geopolymer concrete incorporating alccofine at ambient curing. *Constr. Build. Mater.* **2018**, *180*, 298–307.
63. Shehab, H.K.; Eisa, A.S.; Wahba, A.M. Mechanical properties of fly ash based geopolymer concrete with full and partial cement replacement. *Constr. Build. Mater.* **2016**, *126*, 560–565. [\[CrossRef\]](#)
64. Chithambaram, S.J.; Kumar, S.; Prasad, M.M.; Adak, D. Effect of parameters on the compressive strength of fly ash based geopolymer concrete. *Struct. Concr.* **2018**, *19*, 1202–1209. [\[CrossRef\]](#)
65. Wardhono, A.; Gunasekara, C.; Law, D.W.; Setunge, S. Comparison of long term performance between alkali activated slag and fly ash geopolymer concretes. *Constr. Build. Mater.* **2017**, *143*, 272–279. [\[CrossRef\]](#)
66. Ramujee, K.; PothaRaju, M. Mechanical properties of geopolymer concrete composites. *Mater. Today Proc.* **2017**, *4*, 2937–2945. [\[CrossRef\]](#)
67. Wallah, S.E. Creep behaviour of fly ash-based geopolymer concrete. *Civ. Eng. Dimens.* **2010**, *12*, 73–78.
68. Aliabdo, A.A.; Abd Elmoaty, M.; Salem, H.A. Effect of water addition, plasticizer and alkaline solution constitution on fly ash based geopolymer concrete performance. *Constr. Build. Mater.* **2016**, *121*, 694–703. [\[CrossRef\]](#)
69. Xie, T.; Ozbakkaloglu, T. Behavior of low-calcium fly and bottom ash-based geopolymer concrete cured at ambient temperature. *Ceram. Int.* **2015**, *41*, 5945–5958. [\[CrossRef\]](#)
70. Sarker, P.K. Bond strength of reinforcing steel embedded in fly ash-based geopolymer concrete. *Mater. Struct.* **2011**, *44*, 1021–1030. [\[CrossRef\]](#)
71. Chindaprasirt, P.; Chalee, W. Effect of sodium hydroxide concentration on chloride penetration and steel corrosion of fly ash-based geopolymer concrete under marine site. *Constr. Build. Mater.* **2014**, *63*, 303–310. [\[CrossRef\]](#)
72. Shaikh, F.U.A.; Vimonsatit, V. Compressive strength of fly-ash-based geopolymer concrete at elevated temperatures. *Fire Mater.* **2015**, *39*, 174–188. [\[CrossRef\]](#)
73. Sastry, K.G.K.; Sahitya, P.; Ravitheja, A. Influence of nano TiO₂ on strength and durability properties of geopolymer concrete. *Mater. Today Proc.* **2021**, *45*, 1017–1025. [\[CrossRef\]](#)
74. Çevik, A.; Alzebaree, R.; Humur, G.; Niş, A.; Gülşan, M.E. Effect of nano-silica on the chemical durability and mechanical performance of fly ash based geopolymer concrete. *Ceram. Int.* **2018**, *44*, 12253–12264. [\[CrossRef\]](#)
75. Embong, R.; Kusbiantoro, A.; Shafiq, N.; Nuruddin, M.F. Strength and microstructural properties of fly ash based geopolymer concrete containing high-calcium and water-absorptive aggregate. *J. Clean. Prod.* **2016**, *112*, 816–822. [\[CrossRef\]](#)
76. Sumajouw, D.M.J.; Hardjito, D.; Wallah, S.E.; Rangan, B.V. Fly ash-based geopolymer concrete: Study of slender reinforced columns. *J. Mater. Sci.* **2007**, *42*, 3124–3130. [\[CrossRef\]](#)

77. Jaydeep, S.; Chakravarthy, B.J. Study on fly ash based geo-polymer concrete using admixtures. *Int. J. Eng. Trends Technol.* **2013**, *4*, 4614–4617.
78. Nuaklong, P.; Jongvivatsakul, P.; Pothisiri, T.; Sata, V.; Chindaprasirt, P. Influence of rice husk ash on mechanical properties and fire resistance of recycled aggregate high-calcium fly ash geopolymer concrete. *J. Clean. Prod.* **2020**, *252*, 119797. [\[CrossRef\]](#)
79. Okoye, F.N.; Durgaprasad, J.; Singh, N.B. Effect of silica fume on the mechanical properties of fly ash based-geopolymer concrete. *Ceram. Int.* **2016**, *42*, 3000–3006. [\[CrossRef\]](#)
80. Okoye, F.N.; Prakash, S.; Singh, N.B. Durability of fly ash based geopolymer concrete in the presence of silica fume. *J. Clean. Prod.* **2017**, *149*, 1062–1067. [\[CrossRef\]](#)
81. Sarker, P.K.; Haque, R.; Ramgolam, K.V. Fracture behaviour of heat cured fly ash based geopolymer concrete. *Mater. Des.* **2013**, *44*, 580–586. [\[CrossRef\]](#)
82. Junaid, M.T.; Kayali, O.; Khennane, A. Response of alkali activated low calcium fly-ash based geopolymer concrete under compressive load at elevated temperatures. *Mater. Struct.* **2017**, *50*, 50. [\[CrossRef\]](#)
83. Olivia, M.; Sarker, P.; Nikraz, H. Water penetrability of low calcium fly ash geopolymer concrete. *Proc. ICCBT2008-A* **2008**, *46*, 517–530.
84. Abhilash, P.; Sashidhar, C.; Reddy, I.R. Strength properties of Fly ash and GGBS based Geo-polymer Concrete. *Int. J. ChemTech Res.* **2016**, *17*, 127–135.
85. Jindal, B.B.; Parveen Singhal, D.; Goyal, A. Predicting relationship between mechanical properties of low calcium fly ash-based geopolymer concrete. *Trans. Indian Ceram. Soc.* **2017**, *76*, 258–265. [\[CrossRef\]](#)
86. Vignesh, P.; Vivek, K. An experimental investigation on strength parameters of flyash based geopolymer concrete with GGBS. *Int. Res. J. Eng. Technol.* **2015**, *2*, 135–142.
87. Joseph, B.; Mathew, G. Influence of aggregate content on the behavior of fly ash based geopolymer concrete. *Sci. Iran.* **2012**, *19*, 1188–1194. [\[CrossRef\]](#)
88. Nath, P.; Sarker, P.K. Effect of GGBFS on setting, workability and early strength properties of fly ash geopolymer concrete cured in ambient condition. *Constr. Build. Mater.* **2014**, *66*, 163–171. [\[CrossRef\]](#)
89. Adak, D.; Sarkar, M.; Mandal, S. Structural performance of nano-silica modified fly-ash based geopolymer concrete. *Constr. Build. Mater.* **2017**, *135*, 430–439. [\[CrossRef\]](#)
90. Gunasekara, C.; Law, D.W.; Setunge, S. Long term permeation properties of different fly ash geopolymer concretes. *Constr. Build. Mater.* **2016**, *124*, 352–362. [\[CrossRef\]](#)
91. Mehta, A.; Siddique, R. Sulfuric acid resistance of fly ash based geopolymer concrete. *Constr. Build. Mater.* **2017**, *146*, 136–143. [\[CrossRef\]](#)
92. Cui, Y.; Gao, K.; Zhang, P. Experimental and Statistical Study on Mechanical Characteristics of Geopolymer Concrete. *Materials* **2020**, *13*, 1651. [\[CrossRef\]](#)
93. Albitar, M.; Visintin, P.; Ali, M.M.; Drechsler, M. Assessing behaviour of fresh and hardened geopolymer concrete mixed with class-F fly ash. *KSCE J. Civ. Eng.* **2015**, *19*, 1445–1455. [\[CrossRef\]](#)
94. Bhogayata, A.C.; Arora, N.K. Utilization of metalized plastic waste of food packaging articles in geopolymer concrete. *J. Mater. Cycles Waste Manag.* **2019**, *21*, 1014–1026. [\[CrossRef\]](#)
95. Gomaa, E.; Sargon, S.; Kashosi, C.; Ghenni, A.; ElGawady, M.A. Mechanical Properties of High Early Strength Class C Fly Ash-Based Alkali Activated Concrete. *Transp. Res. Rec.* **2020**, *2674*, 430–443. [\[CrossRef\]](#)
96. Hassan, A.; Arif, M.; Shariq, M. Effect of curing condition on the mechanical properties of fly ash-based geopolymer concrete. *SN Appl. Sci.* **2019**, *1*, 1694. [\[CrossRef\]](#)
97. Kurtoglu, A.E.; Alzebaree, R.; Aljumaili, O.; Nis, A.; Gulsan, M.E.; Humur, G.; Cevik, A. Mechanical and durability properties of fly ash and slag based geopolymer concrete. *Adv. Concr. Constr.* **2018**, *6*, 345.
98. Nath, P.; Sarker, P.K. Use of OPC to improve setting and early strength properties of low calcium fly ash geopolymer concrete cured at room temperature. *Cem. Concr. Compos.* **2015**, *55*, 205–214. [\[CrossRef\]](#)
99. Saravanan, S.; Elavenil, S. Strength Properties of Geopolymer Concrete using M Sand by Assessing their Mechanical Characteristics. *ARPN J. Eng. Appl. Sci.* **2018**, *13*, 4028–4041.
100. Topark-Ngarm, P.; Chindaprasirt, P.; Sata, V. Setting time, strength, and bond of high-calcium fly ash geopolymer concrete. *J. Mater. Civ. Eng.* **2015**, *27*, 04014198. [\[CrossRef\]](#)
101. Vijai, K.; Kumutha, R.; Vishnuram, B.G. Experimental Investigations on Mechanical Properties of Geopolymer Concrete Composites. 2011. Available online: <http://dl.lib.mrt.ac.lk/handle/123/9265> (accessed on 17 October 2021).
102. Vora, P.R.; Dave, U.V. Parametric studies on compressive strength of geopolymer concrete. *Procedia Eng.* **2013**, *51*, 210–219. [\[CrossRef\]](#)
103. Wang, Y.; Hu, S.; He, Z. Mechanical and Fracture Properties of Fly Ash Geopolymer Concrete Addictive with Calcium Aluminate Cement. *Materials* **2019**, *12*, 2982. [\[CrossRef\]](#)
104. Ibrahim, M.; Johari, M.A.M.; Maslehuddin, M.; Rahman, M.K. Influence of nano-SiO₂ on the strength and microstructure of natural pozzolan based alkali activated concrete. *Constr. Build. Mater.* **2018**, *173*, 573–585. [\[CrossRef\]](#)
105. Ghafoor, M.T.; Khan, Q.S.; Qazi, A.U.; Sheikh, M.N.; Hadi, M.N.S. Influence of alkaline activators on the mechanical properties of fly ash based geopolymer concrete cured at ambient temperature. *Constr. Build. Mater.* **2021**, *273*, 121752. [\[CrossRef\]](#)

106. Fang, G.; Ho, W.K.; Tu, W.; Zhang, M. Workability and mechanical properties of alkali-activated fly ash-slag concrete cured at ambient temperature. *Constr. Build. Mater.* **2018**, *172*, 476–487. [\[CrossRef\]](#)
107. Vijai, K.; Kumutha, R.; Vishnuram, B.G. Effect of types of curing on strength of geopolymer concrete. *Int. J. Phys. Sci.* **2010**, *5*, 1419–1423.
108. Krishnaraja, A.R.; Sathishkumar, N.P.; Kumar, T.S.; Kumar, P.D. Mechanical behaviour of geopolymer concrete under ambient curing. *Int. J. Sci. Eng. Technol.* **2014**, *3*, 130–132.
109. Kumaravel, S. Development of various curing effect of nominal strength Geopolymer concrete. *J. Eng. Sci. Technol. Rev.* **2014**, *7*, 116–119. [\[CrossRef\]](#)
110. Nagajothi, S.; Elavenil, S. Effect of GGBS Addition on Reactivity and Microstructure Properties of Ambient Cured Fly Ash Based Geopolymer Concrete. *Silicon* **2021**, *13*, 507–516. [\[CrossRef\]](#)
111. Muhammad, N.; Baharom, S.; Ghazali, N.A.M.; Alias, N.A. Effect of Heat Curing Temperatures on Fly Ash-Based Geopolymer Concrete. *Int. J. Eng. Technol.* **2019**, *8*, 15–19.
112. Das, S.K.; Shrivastava, S. Siliceous fly ash and blast furnace slag based geopolymer concrete under ambient temperature curing condition. *Struct. Concr.* **2020**, *22*, E341–E351. [\[CrossRef\]](#)
113. Nuruddin, M.N.; Kusbiantoro, A.K.; Qazi, S.Q.; Darmawan, M.D.; Husin, N.H. Development of geopolymer concrete with different curing conditions. *IPTEK J. Technol. Sci.* **2011**, *22*, 24–28. [\[CrossRef\]](#)
114. Ramujee, K. Development of low calcium flyash based geopolymer concrete. *Int. J. Eng. Technol.* **2014**, *6*, 1. [\[CrossRef\]](#)
115. Mohammed, A.; Rafiq, S.; Sihag, P.; Kurda, R.; Mahmood, W.; Ghafor, K.; Sarwar, W. ANN, M5P-tree and nonlinear regression approaches with statistical evaluations to predict the compressive strength of cement-based mortar modified with fly ash. *J. Mater. Res. Technol.* **2020**, *9*, 12416–12427. [\[CrossRef\]](#)
116. Thakur, R.N.; Ghosh, S. Effect of mix composition on compressive strength and microstructure of fly ash based geopolymer composites. *ARPN J. Eng. Appl. Sci.* **2009**, *4*, 68–74.
117. Dombrowski, K.; Buchwald, A.; Weil, M. The influence of calcium content on the structure and thermal performance of fly ash based geopolymers. *J. Mater. Sci.* **2007**, *42*, 3033–3043. [\[CrossRef\]](#)
118. Chi, M.; Huang, R. Binding mechanism and properties of alkali-activated fly ash/slag mortars. *Constr. Build. Mater.* **2013**, *40*, 291–298. [\[CrossRef\]](#)
119. Fernandez-Jimenez, A.M.; Palomo, A.; Lopez-Hombrados, C. Engineering properties of alkali-activated fly ash concrete. *ACI Mater. J.* **2006**, *103*, 106.
120. Ryu, G.S.; Lee, Y.B.; Koh, K.T.; Chung, Y.S. The mechanical properties of fly ash-based geopolymer concrete with alkaline activators. *Constr. Build. Mater.* **2013**, *47*, 409–418. [\[CrossRef\]](#)
121. Khale, D.; Chaudhary, R. Mechanism of geopolymerization and factors influencing its development: A review. *J. Mater. Sci.* **2007**, *42*, 729–746. [\[CrossRef\]](#)
122. Thokchom, S.; Mandal, K.K.; Ghosh, S. Effect of Si/Al ratio on performance of fly ash geopolymers at elevated temperature. *Arab. J. Sci. Eng.* **2012**, *37*, 977–989. [\[CrossRef\]](#)
123. Garcia-Lodeiro, I.; Palomo, A.; Fernández-Jiménez, A.; Macphee, D.E. Compatibility studies between NASH and CASH gels. Study in the ternary diagram $\text{Na}_2\text{O}-\text{CaO}-\text{Al}_2\text{O}_3-\text{SiO}_2-\text{H}_2\text{O}$. *Cem. Concr. Res.* **2011**, *41*, 923–931. [\[CrossRef\]](#)
124. Faraj, R.H.; Mohammed, A.A.; Mohammed, A.; Omer, K.M.; Ahmed, H.U. Systematic multiscale models to predict the compressive strength of self-compacting concretes modified with nanosilica at different curing ages. *Eng. Comput.* **2021**, *29*, 1–24. [\[CrossRef\]](#)
125. Sathonsaowaphak, A.; Chindaprasirt, P.; Pimraksa, K. Workability and strength of lignite bottom ash geopolymer mortar. *J. Hazard. Mater.* **2009**, *168*, 44–50. [\[CrossRef\]](#)
126. Rafeet, A.; Vinai, R.; Soutsos, M.; Sha, W. Guidelines for mix proportioning of fly ash/GGBS based alkali activated concretes. *Constr. Build. Mater.* **2017**, *147*, 130–142. [\[CrossRef\]](#)
127. Lloyd, R.R.; Provis, J.L.; van Deventer, J.S. Microscopy and microanalysis of inorganic polymer cements. 1: Remnant fly ash particles. *J. Mater. Sci.* **2009**, *44*, 608–619. [\[CrossRef\]](#)
128. Hu, W.; Nie, Q.; Huang, B.; Su, A.; Du, Y.; Shu, X.; He, Q. Mechanical property and microstructure characteristics of geopolymer stabilized aggregate base. *Constr. Build. Mater.* **2018**, *191*, 1120–1127. [\[CrossRef\]](#)
129. Deb, P.S.; Nath, P.; Sarker, P.K. The effects of ground granulated blast-furnace slag blending with fly ash and activator content on the workability and strength properties of geopolymer concrete cured at ambient temperature. *Mater. Des. (1980–2015)* **2014**, *62*, 32–39. [\[CrossRef\]](#)
130. Hardjito, D.; Wallah, S.E.; Sumajouw, D.M.; Rangan, B.V. On the development of fly ash-based geopolymer concrete. *Mater. J.* **2004**, *101*, 467–472.
131. Barbosa, V.F.; MacKenzie, K.J.; Thaumaturgo, C. Synthesis and characterisation of materials based on inorganic polymers of alumina and silica: Sodium polysialate polymers. *Int. J. Inorg. Mater.* **2000**, *2*, 309–317. [\[CrossRef\]](#)
132. Patankar, S.V.; Jamkar, S.S.; Ghugal, Y.M. Effect of water-to-geopolymer binder ratio on the production of fly ash based geopolymer concrete. *Int. J. Adv. Technol. Civ. Eng.* **2013**, *2*, 79–83.
133. Van Jaarsveld, J.G.S.; Van Deventer, J.S.J.; Lukey, G.C. The effect of composition and temperature on the properties of fly ash-and kaolinite-based geopolymers. *Chem. Eng. J.* **2002**, *89*, 63–73. [\[CrossRef\]](#)

134. He, J.; Jie, Y.; Zhang, J.; Yu, Y.; Zhang, G. Synthesis and characterization of red mud and rice husk ash-based geopolymer composites. *Cem. Concr. Compos.* **2013**, *37*, 108–118. [\[CrossRef\]](#)
135. Rickard, W.D.; Williams, R.; Temuujin, J.; Van Riessen, A. Assessing the suitability of three Australian fly ashes as an aluminosilicate source for geopolymers in high temperature applications. *Mater. Sci. Eng. A* **2011**, *528*, 3390–3397. [\[CrossRef\]](#)
136. Komljenović, M.; Baščarević, Z.; Bradić, V. Mechanical and microstructural properties of alkali-activated fly ash geopolymers. *J. Hazard. Mater.* **2010**, *181*, 35–42. [\[CrossRef\]](#)
137. Kumar, S.; Kumar, R. Mechanical activation of fly ash: Effect on reaction, structure and properties of resulting geopolymer. *Ceram. Int.* **2011**, *37*, 533–541. [\[CrossRef\]](#)
138. ASTM-C33. *Standard Specification for Concrete Aggregates*; ASTM International: West Conshohocken, PA, USA, 2016.
139. Mermerdaş, K.; Manguri, S.; Nassani, D.E.; Oleiwi, S.M. Effect of aggregate properties on the mechanical and absorption characteristics of geopolymer mortar. *Eng. Sci. Technol. Int. J.* **2017**, *20*, 1642–1652. [\[CrossRef\]](#)
140. Mane, S.; Jadhav, H.S. Investigation of geopolymer mortar and concrete under high temperature. *Int. J. Emerg. Technol. Adv. Eng.* **2012**, *2*, 384–390.
141. Nuaklong, P.; Sata, V.; Chindaprasirt, P. Influence of recycled aggregate on fly ash geopolymer concrete properties. *J. Clean. Prod.* **2016**, *112*, 2300–2307. [\[CrossRef\]](#)
142. Sreenivasulu, C.; Guru, J.J.; Sekhar, R.M.V.; Pavan, K.D. Effect of fine aggregate blending on short-term mechanical properties of geopolymer concrete. *Asian J. Civ. Eng.* **2016**, *17*, 537–550.
143. Puligilla, S.; Mondal, P. Role of slag in microstructural development and hardening of fly ash-slag geopolymer. *Cem. Concr. Res.* **2013**, *43*, 70–80. [\[CrossRef\]](#)
144. Nath, P.; Sarker, P.K. Flexural strength and elastic modulus of ambient-cured blended low-calcium fly ash geopolymer concrete. *Constr. Build. Mater.* **2017**, *130*, 22–31. [\[CrossRef\]](#)
145. Weng, L.; Sagoe-Crentsil, K. Dissolution processes, hydrolysis and condensation reactions during geopolymer synthesis: Part I—Low Si/Al ratio systems. *J. Mater. Sci.* **2007**, *42*, 2997–3006. [\[CrossRef\]](#)
146. Sagoe-Crentsil, K.; Weng, L. Dissolution processes, hydrolysis and condensation reactions during geopolymer synthesis: Part II. High Si/Al ratio systems. *J. Mater. Sci.* **2007**, *42*, 3007–3014. [\[CrossRef\]](#)
147. Mustafa Al Bakri, A.M.; Kamarudin, H.; Bnhussain, M.; Rafiza, A.R.; Zarina, Y. Effect of Na₂SiO₃/NaOH Ratios and NaOH Molarities on Compressive Strength of Fly-Ash-Based Geopolymer. *ACI Mater. J.* **2012**, *109*, 503–508.
148. Ridditirud, C.; Chindaprasirt, P.; Pimraksa, K. Factors affecting the shrinkage of fly ash geopolymers. *Int. J. Miner. Metall. Mater.* **2011**, *18*, 100–104. [\[CrossRef\]](#)
149. Phoo-ngernkham, T.; Maegawa, A.; Mishima, N.; Hatanaka, S.; Chindaprasirt, P. Effects of sodium hydroxide and sodium silicate solutions on compressive and shear bond strengths of FA-GBFS geopolymer. *Constr. Build. Mater.* **2015**, *91*, 1–8. [\[CrossRef\]](#)
150. Morsy, M.S.; Alsayed, S.H.; Al-Salloum, Y.; Almusallam, T. Effect of sodium silicate to sodium hydroxide ratios on strength and microstructure of fly ash geopolymer binder. *Arab. J. Sci. Eng.* **2014**, *39*, 4333–4339. [\[CrossRef\]](#)
151. Alonso, S.; Palomo, A. Alkaline activation of metakaolin and calcium hydroxide mixtures: Influence of temperature, activator concentration and solids ratio. *Mater. Lett.* **2001**, *47*, 55–62. [\[CrossRef\]](#)
152. Varaprasad, B.S.K.R.J.; Reddy, K.N.K. Strength and workability of low lime fly-ash based geopolymer concrete. *Indian J. Sci. Technol.* **2010**, *3*, 1188–1189.
153. Chindaprasirt, P.; Chareerat, T.; Hatanaka, S.; Cao, T. High-strength geopolymer using fine high-calcium fly ash. *J. Mater. Civ. Eng.* **2011**, *23*, 264–270. [\[CrossRef\]](#)
154. Duxson, P.; Lukey, G.C.; Separovic, F.; Van Deventer, J.S.J. Effect of alkali cations on aluminum incorporation in geopolymeric gels. *Ind. Eng. Chem. Res.* **2005**, *44*, 832–839. [\[CrossRef\]](#)
155. Görhan, G.; Kürklü, G. The influence of the NaOH solution on the properties of the fly ash-based geopolymer mortar cured at different temperatures. *Compos. Part B Eng.* **2014**, *58*, 371–377. [\[CrossRef\]](#)
156. ACI Committee 211.1. *Standard Practice for Selecting Proportions for Normal, Heavyweight, and Mass Concrete (ACI 211.1R-02)*; American Concrete Institute: Farmington Hills, MI, USA, 2002.
157. Darabi, M.K.; Huang, C.W.; Bazzaz, M.; Masad, E.A.; Little, D.N. Characterization and validation of the nonlinear viscoelastic-viscoplastic with hardening-relaxation constitutive relationship for asphalt mixtures. *Constr. Build. Mater.* **2019**, *216*, 648–660. [\[CrossRef\]](#)
158. Bazzaz, M.; Darabi, M.K.; Little, D.N.; Garg, N. A straightforward procedure to characterize nonlinear viscoelastic response of asphalt concrete at high temperatures. *Transp. Res. Rec.* **2018**, *2672*, 481–492. [\[CrossRef\]](#)
159. Bazzaz, M.; Darabi, M.K.; Little, D.N.; Garg, N. Effect of evotherm-M1 on properties of asphaltic materials used at NAPMRC testing facility. *J. Test. Eval.* **2019**, *48*, 2256–2269. [\[CrossRef\]](#)
160. Abdullah, W.A.; Ahmed, H.U.; Alshkane, Y.M.; Rahman, D.B.; Ali, A.O.; Abubakr, S.S. The Possibility of Using Waste PET Plastic Strip to Enhance the Flexural Capacity of Concrete Beams. *J. Eng. Res.* **2021**, *9*, 1–17. [\[CrossRef\]](#)